SCF^{Slmb} recognizes a conserved degron within the survival motor neuron (SMN) self-interaction domain to mediate ubiquitylation of SMN and SMNΔ7 isoforms

Kelsey M. Gray[a], Kevin A. Kaifer[b], David Baillat[c], Ying Wen[a], Jacqueline J. Glascock[b], Allison D. Ebert[d], Sara ten Have[e], Angus I. Lamond[e], Eric J. Wagner[c], Christian L. Lorson[b], and A. Gregory Matera[a]

Running title: SCF^{Slmb} mediates degradation of SMN

[a]Curriculum in Genetics and Molecular Biology, Integrative Program in Biological and Genome Sciences, Departments of Biology and Genetics, University of North Carolina, Chapel Hill, NC 27599, USA

[b]Molecular Pathogeneses and Therapeutics Program, Department of Veterinary Pathobiology, College of Veterinary Medicine, Bond Life Sciences Center, University of Missouri, Columbia, MO 65211, USA

[c]Department of Biochemistry and Molecular Biology, University of Texas Medical Branch, Galveston, TX 77550, USA

[d]Department of Cell Biology, Neurobiology and Anatomy, Medical College of Wisconsin, 8701 Watertown Plank Rd, Milwaukee, WI 53226, USA

[e]Centre for Gene Regulation and Expression, School of Life Sciences, University of Dundee, Dundee, DD15EH, UK

Address correspondence to: A. Gregory Matera
Integrative Program for Biological and Genome Sciences
Campus Box 7100
University of North Carolina
Chapel Hill, NC 27599
Voice: (919) 962-4567
FAX: (919) 962-4574

Abstract

Spinal muscular atrophy (SMA) is caused by homozygous loss of human *SMN1 (survival motor neuron 1)*. Expression of a duplicate gene *(SMN2)* primarily results in skipping of exon 7 and production of an unstable protein, called SMNΔ7. Although *SMN2* exon skipping is the principal contributor to SMA severity, mechanisms governing stability of SMN protein isoforms are poorly understood. We used a *Drosophila* model system and 'label-free' proteomics to identify the SCF^{Slmb} ubiquitin E3 ligase complex as a novel SMN binding partner. We show that this interaction is conserved from fly to human, and that SCF^{Slmb} interacts with a phospho-degron embedded within the SMN YG-box self-oligomerization domain. Substitution of a conserved serine (S270A) interferes with SCF^{Slmb} binding and greatly stabilizes SMNΔ7. SMA-causing missense mutations that block multimerization of full-length SMN are also stabilized in the degron mutant background. Furthermore, overexpression of $SMN\Delta7^{S270A}$, but not wild-type SMNΔ7, provides a protective effect in SMA model mice and human motor neuron cell culture systems. Our findings support a model wherein the SCF^{Slmb} degron is largely exposed when SMN is monomeric, whereas it is sequestered when SMN forms higher-order multimers. SMN stability is thus regulated by self-oligomerization, providing an elegant mechanism for balancing functional activity.

Introduction

Spinal muscular atrophy (SMA) is a common neuromuscular disorder, recognized as the most prevalent genetic cause of early childhood mortality (Pearn 1980). Patients with the most severe form of the disease, which is also the most common, become symptomatic in the first six months of life and rarely live past two years (Wee et al. 2010; Prior 2010). Because the onset of symptoms and their severity can vary, SMA has historically been classified into three subtypes (Ogino and Wilson 2004). More recently, clinicians have recognized that SMA is better characterized as a continuous spectrum disorder, ranging from acute (prenatal onset) to nearly asymptomatic (Tiziano et al. 2013). Clinically, SMA patients experience degeneration of motor neurons in the anterior horn of the lower spinal cord (Crawford and Pardo 1996). This leads to progressive atrophy of proximal muscle groups, ultimately resulting in loss of motor function and symmetrical paralysis. The cause of death is often restrictive respiratory failure (Kolb and Kissell 2015).

SMA typically results from homozygous deletion of the *survival motor neuron 1* (*SMN1*) gene (Lefebvre et al. 1995). A small fraction of SMA patients have lost one copy of *SMN1* and the remaining copy contains a point mutation (Burghes and Beattie 2009). Humans have two *SMN* paralogs, named *SMN1* and *SMN2*, both of which contribute to total cellular levels of SMN protein. *SMN2* exon 7 contains a silent base change that alters splicing to primarily produce a truncated, unstable protein product called SMNΔ7 (Lorson et al. 1999; Monani et al. 1999; Lorson and Androphy 2000). The last 16 amino acids of SMN are replaced in SMNΔ7 by four amino acids, EMLA, encoded by exon 8. Current estimates suggest that *SMN2* produces 10-15% of the level of full-length protein produced by *SMN1* (Lorson et al. 2010). Complete loss of SMN is lethal in all organisms investigated to date (Schrank et al. 1997; Monani 2005). Although the amount of full-length protein produced by *SMN2* is not enough to compensate for loss of *SMN1*, *SMN2* is sufficient to rescue embryonic lethality (Monani et al. 2000). SMA is therefore a disease that arises due to a hypomorphic reduction in SMN levels (Lefebvre et al. 1995). Furthermore, relative levels of the SMN protein correlate with the phenotypic severity of SMA (Coovert et al. 1997; Lefebvre et al. 1997).

Whereas a causative link between *SMN1* and SMA was established over 20 years ago, the molecular role of SMN in disease etiology remains unclear. SMN is the central component of a multimeric protein assemblage known as the SMN complex (Matera and

Wang 2014; Li et al. 2014). The best-characterized function of this complex, which is found in all tissues of metazoan organisms, is in the cytoplasmic assembly of small nuclear ribonucleoproteins (snRNPs), core components of the spliceosome (Fischer et al. 1997; Meister et al. 2001; Pellizzoni et al. 2002).

Although it is ubiquitously expressed, SMN has also been implicated in a number of tissue-specific processes related to neurons and muscles. These functions include actin dynamics (Oprea et al. 2008; Ackermann et al. 2013), axonal pathfinding (Fan and Simard 2002; McWhorter et al. 2003; Sharma et al. 2005), axonal transport of β-actin mRNP (Rossoll et al. 2003), phosphatase and tensin homolog-mediated (PTEN-mediated) protein synthesis pathways (Ning et al. 2010), translational regulation (Sanchez et al. 2013), neuromuscular junction formation and function (Chan et al. 2003; Kariya et al. 2008; Kong et al. 2009; Voigt et al. 2010), myoblast fusion (Shafey et al. 2005) and maintenance of muscle architecture (Rajendra et al. 2007; Walker et al. 2008; Bowerman et al. 2009).

Ubiquitylation pathways have been shown to regulate the stability and degradation of SMN (Chang et al. 2004; Burnett et al. 2009; Hsu et al. 2010) as well as axonal and synaptic stability (Korhonen and Lindholm 2004). In the ubiquitin proteasome system (UPS), proteins destined for degradation are tagged by linkage to ubiquitin through the action of three factors (Petroski 2008). E1 proteins activate ubiquitin and transfer it to the E2 enzyme. E2 proteins conjugate ubiquitin to their substrates. E3 proteins recognize the substrate and assist in the transfer of ubiquitin from the E2. Because E3 ligases confer substrate specificity, they are typically considered as candidates for targeted inhibition of protein degradation. Ubiquitin homeostasis is thought to be particularly important for neuromuscular pathology in SMA (Groen and Gillingwater 2015). Indeed, mouse models of SMA display widespread perturbations in UBA1 (ubiquitin-like modifier activating enzyme 1) levels (Wishart et al. 2014). Furthermore, mutations in UBA1 are known to cause X-linked infantile SMA (Ramser et al. 2008; Schmutzler et al. 2008).

Given the importance of these processes to normal development as well as neurodegenerative disease, we set out to identify and characterize novel SMN binding partners. Previously, we developed *Drosophila* as a model system wherein the endogenous *Smn* gene is replaced with a *Flag-Smn* transgene (Praveen et al. 2012). When expressed in the fly, SMA-causing point mutations recapitulate the full range of

phenotypic severity seen in humans (Praveen et al. 2014; Garcia et al. 2016). Using this system, we carried out proteomic profiling of Flag-purified embryonic lysates and identified the SCF^{Slmb} E3 ubiquitin ligase complex as a novel SMN interactor. Importantly, this interaction is conserved from flies to humans. We show that SCF^{Slmb} binding requires a phospho-degron motif located within the SMN self-oligomerization domain, whose mutation stabilizes both SMNΔ7 and full-length SMN. Additional studies in flies, mice and human cells elucidate a disease-relevant mechanism whereby SMN protein stability is regulated by self-oligomerization.

Results

Flag-SMN interacts with UPS (ubiquitin proteasome system) proteins

We previously generated transgenic *Drosophila melanogaster* that express Flag-tagged SMN proteins in an otherwise null *Smn* background (Praveen et al. 2012). To preserve endogenous expression patterns, the constructs are driven by the native promoter and flanking sequences. As described in the Methods, we intercrossed hemizygous *Flag-*Smn^{WT},Smn^{X7}/Smn^{D} animals to establish a stock wherein all of the SMN protein, including the maternal contribution, is epitope-tagged. After breeding them for >100 generations, essentially all of the animals are homozygous for the *Flag-*Smn^{WT} transgene, but second site recessives are minimized due to the use of two different *Smn* null alleles. Adults from this stock display no apparent defects and have an eclosion frequency (~90%) similar to that of wild-type (Oregon-R) animals.

We collected (0-12h) embryos from *Flag-*Smn^{WT} (SMN) and Oregon-R (Ctrl) animals and analyzed Flag-purified lysates by 'label-free' mass spectrometry. In addition to Flag-SMN, we identified SMN complex components Gemin2 and Gemin3, along with all seven of the canonical Sm-core snRNP proteins (Fig. 1A). We also identified the U7-specific Sm-like heterodimer Lsm10/11 (Pillai et al. 2003) and the Gemin5 orthologue, Rigor mortis (Gates et al. 2004). Previous studies of Schneider2 (S2) cells transfected with epitope-tagged *Smn* had identified most of the proteins listed above as SMN binding partners in *Drosophila* (Kroiss et al. 2008). However, despite bioinformatic (Kroiss et al. 2008) and cell biological (Cauchi et al. 2010) data indicating that Rigor mortis is part of the fruit fly SMN complex, this protein failed to co-purify with SMN in S2 cells (Kroiss et

al. 2008; Guruharsha et al. 2011). On the basis of these data, we conclude that our purification conditions are effective and that Rigor mortis/Gemin5 is an integral member of the SMN complex in flies.

In addition to SMN complex members, we also co-purified numerous factors that are part of the ubiquitin proteasome system (UPS; Fig. 1B). Among these UPS proteins, we identified Cullin 1 (Cul1), Skp1-related A (SkpA), and supernumerary limbs (Slmb), as being highly enriched (>10 fold) in Flag-SMN samples as compared to the controls. Together, these proteins comprise the SCF^{Slmb} E3 ubiquitin ligase. Cul1 forms the major structural scaffold of this horseshoe-shaped, multi-subunit complex (Zheng et al. 2002). Slmb is a F-box protein and is the substrate recognition component (Jiang and Struhl 1998). SkpA is a bridging protein essential for interaction of Cul1 with the F-box protein (Patton et al. 1998a; Patton et al. 1998b). Because of its role in substrate recognition, Slmb is likely to be the direct interacting partner of SMN within the SCF^{Slmb} complex. For this reason, we focused on Slmb for the initial verification. As shown, Slmb was easily detectable in Flag-purified eluates from embryos expressing Flag-SMN and nearly undetectable in those from control embryos (Fig. 1C).

SCF^{Slmb} is a *bona fide* SMN protein interaction partner

The interaction of SCF^{Slmb} with SMN was further verified in a reciprocal co-immunoprecipitation demonstrating that Flag-tagged SCF components form complexes with Myc-SMN and endogenous SMN in S2 cells (Fig. 2A). We also tested SMN interaction with Roc1a, a RING domain protein known to interact with Cul1 (Noureddine et al. 2002). SMN was clearly detected following immunoprecipitation of Cul1-Flag and Flag-Slmb (Fig. 2A), and we also detected slightly above background levels after immunoprecipitation of Flag-Roc1a and SkpA-Flag. Notably, when probed with anti-SMN antibodies, Flag-Slmb reproducibly co-precipitates four higher molecular weight species of SMN (Fig. 2B). The steps of the ladder are separated by ~8kDa, which is very close to the MW of ubiquitin. Furthermore, this ladder is not visible following immunoprecipitation by Gemin2 or any of the other SCF^{Slmb} components, which are not expected to be direct binding partners of ubiquitylated SMN. These findings suggest that Slmb associates with mono-, di-, tri-, and tetra-ubiquityltated SMN isoforms.

The SCF complex is highly conserved from flies to humans: SkpA is 77% identical to human Skp1, Cul1 is 63% identical, and Slmb is 80% identical to its human homologs, B-TrCP1 and B-TrCP2. We therefore tested the interaction of Flag-tagged *Drosophila* SCF components with endogenous human SMN in HEK 293T cells (Fig. 2C). Accordingly, human SMN was co-precipitated with Flag-Cul1 and Flag-Slmb and at lower levels following Flag-SkpA immunoprecipitation. Finally, we detected interaction of Flag-B-TrCP1 and Flag-B-TrCP2, the two human homologs of Slmb, with endogenous human SMN in HEK 293T cells (Fig. 2D). Altogether, these data demonstrate a conserved interaction between SMN and the $SCF^{Slmb/B\text{-}TrCP}$ E3 ubiquitin ligase complex.

Depletion of Slmb/B-TrCP results in modest increase of SMN levels

Given that one of the primary functions of protein ubiquitylation is to target proteins to the proteasome for degradation, we examined whether depletion of Slmb by RNAi using dsRNA in S2 cells would result in increased SMN levels (Fig. 3A). Following Slmb RNAi, endogenous SMN levels were modestly increased as compared to cells treated with control dsRNA. We obtained similar results using an siRNA that targets both B-TrCP1 and B-TrCP2 in HeLa cells. As shown in Fig. 3B, we detected a modest increase in levels of full-length SMN following B-TrCP RNAi, but not control RNAi. Next, we treated S2 cells with cycloheximide (CHX), in the presence or absence of dsRNA targeting Slmb, to determine whether differences in SMN levels would be exacerbated when production of new proteins was prevented (Fig. 3C). At 6 hours post-CHX treatment there is a modest increase in full-length SMN levels following Slmb RNAi as compared to the initial timepoint (0h) or the negative control (Osk) RNAi (Fig. 3C). Together, these data indicate that Slmb/B-TrCP participates in the regulation of SMN protein levels.

Identification and characterization of a Slmb/B-TrCP degradation signal in SMN

Studies of numerous UPS substrates in a variety of species have revealed the presence of degradation signals (called degrons) that are required for proper E3 target recognition and binding. Slmb/B-TrCP canonically recognizes a consensus DpSGXXpS/T degron, where p indicates a phosphoryl group (Jin et al. 2005; Frescas and Pagano 2008; Fuchs et al. 2004). There are also several known variants of this motif, for example: DDGFVD, SSGYFS, TSGCSS (Kim et al. 2015). As shown in Fig. 4A, we identified a putative Slmb/B-TrCP degron (^{269}MSGYHT^{274}) in the highly conserved self-oligomerization

domain (YG Box) of SMN. Interestingly, this sequence was previously identified as part of larger degron motif (^{268}YMSGYHTGYYMEMLA^{282}) that was thought to be created in SMNΔ7 by *SMN2* alternative splicing (Cho and Dreyfuss 2010). In particular, mutation of S270 (S201 in flies) to alanine was shown to dramatically stabilize SMNΔ7 constructs in human cells, and overexpression of SMNΔ7^{S270A} in SMN-deficient chicken DT40 cells rescued their viability (Cho and Dreyfuss 2010). However, factors responsible for specifically mediating SMNΔ7 degradation have not been identified.

In order to develop a more SMA-relevant *Drosophila* system with which to investigate SMN YG box function, we generated a 'vertebrate-like' SMN backbone, called vSmn (Fig. 4A). This construct is fully functional *in vivo* (see below). We then generated serine to alanine mutations in both the full-length (vSmnS201A) and truncated (vSmnΔ7A) versions of the protein. To test the effects of overall protein length and distance of the putative degron from the C-terminus, we also generated SMN constructs that are the same length as SMNΔ7, replacing MEMLA* (the amino acids introduced by human *SMN2* splicing) with MGLRQ*, see Fig. 4A. The S201A mutation was created in this construct as well (MGLRQ*^{S201A}). To mimic a constitutively phosphorylated state, we also generated vSmn^{S201D} and vSmnΔ7D. We transfected each of these constructs, Flag-tagged and driven by the native *Smn* promoter, into S2 cells and measured protein levels by western blotting (Fig. 4B). As shown, the constructs that contain the S201A mutation exhibited increased protein levels whereas those of the S201D mutants were comparable or slightly reduced, suggesting that the phospho-degron motif identified in human SMNΔ7 (Cho and Dreyfuss 2010) is also conserved in the fly protein.

We note that the MGLRQ* construct is present at levels that are similar to wild-type (vSmn) and much higher than vSmnΔ7S. Based on the crystal structures of the SMN YG box (Martin et al. 2012; Gupta et al. 2015), the presence of the MGLR insertion in *Drosophila* SMN is predicted to promote self-oligomerization (A.G.M. and G.D. Van Duyne, unpublished), thus stabilizing the protein within the SMN complex (Burnett et al. 2009). By the same logic, the relative inability of vSmnΔ7S to self-interact would be predicted to lead to its destruction. To determine whether the observed increase in SMN protein levels correlated with its ability to interact with Slmb, we co-transfected the appropriate Flag-Smn constructs with Myc-Slmb in S2 cells. Protein lysates were then

Flag-immunoprecipitated and probed with anti-Myc antibody (Fig. 4C). The S201A mutation decreased binding of Slmb to both the full-length and the truncated SMN isoforms (Fig. 4C). However, the vSmnΔ7S construct co-precipitated the greatest amount of Slmb protein, despite the fact that it is present at much lower levels in the input lysate (Fig. 4C). Because SMNΔ7 is defective in self-interaction, this result suggests that the degron is more accessible to Slmb when SMN is monomeric and cannot efficiently oligomerize.

SMN self-oligomerization regulates access to the Slmb degron

To examine the connection between SMN self-oligomerization and degron accessibility more closely we took advantage of two YG box point mutations (Y203C and G206S) that are known to destabilize the full-length protein and to decrease its self-oligomerization capacity (Praveen et al. 2014). As a control, we also employed a mutation (G210V) that does not disrupt self-oligomerization (Praveen et al. 2014; Gupta et al. 2015). Next, we introduced the S201A mutation into all three of these full-length SMN constructs, transfected them into S2 cells and carried out western blotting to detect levels of each transfected construct (Fig. 5A). As quantified in Fig. 5B, the S201A degron mutation has a clear stabilizing effect on the G206S and Y203C constructs, as compared to the effect of S201A paired with G210V. Hence, we conclude that the Slmb degron is exposed when SMN is present predominantly as a monomer, whereas it is less accessible when the protein is able to form higher order multimers.

SMNΔ7A is a protective modifier of intermediate SMA phenotypes

Increased *SMN2* copy number, and therefore increased SMNΔ7 protein, correlates with a milder clinical phenotype in SMA patients (Wirth 2000). This phenomenon was successfully modeled in mice over a decade ago (Monani et al. 2000; Hsieh-Li et al. 2000), showing that high copy number *SMN2* transgenes fully rescue the null phenotype, whereas low copy transgenes do not. Moreover, transgenic expression of a human SMNΔ7 cDNA construct in a low-copy *SMN2* background improves survival of this severe SMA mouse model from P5 (post-natal day 5) to P13 (Le et al. 2005). Experiments in an SMN-deficient DT40 cell line showed that expression of SMNΔ7A, but not SMNΔ7S, rescued cellular proliferation (Cho and Dreyfuss 2010), demonstrating that SMNΔ7A is at least partially functional.

To examine whether expression of SMNΔ7A could rescue animal development, we generated flies carrying Flag-tagged vSmnΔ7A and vSmnS201A transgenes in an otherwise null *Smn* background. As shown in Fig. S1, levels of vSmnΔ7A were very low, and that of the vSmnΔ7S transgene was barely detectable in comparison to the full-length constructs. Levels of vSmn and vSmn^{S201A} were comparable and, as expected, both transgenes produce fully viable and fertile adults (Fig. 6A). In fact, the eclosion frequencies of animals expressing Flag-vSmn or -vSmn^{S201A} are higher than those of wild-type Flag-Smn (Fig. 6A and Praveen et al. 2012; Praveen et al. 2014). In contrast, neither Flag-vSmnΔ7S nor -vSmnΔ7A was able to rescue viability of the *Smn* null allele; these animals also died as late 2nd or early 3rd instar larvae. We crossed the Flag-vSmnΔ7S nor -vSmnΔ7A transgenes with *Smn* alleles of varying severity, as determined by protein levels (Praveen et al. 2014). These include, in order of decreasing severity: a V72G point mutant (V72G), a wild-type Flag-Smn line that expresses lower than endogenous levels of SMN (WT), and a balancer chromosome (+) that expresses normal levels of SMN. When crossed to each of these allelic combinations (Fig. 6B), the constructs did not provide a protective benefit. Thus, we conclude that transgenic expression of Flag-vSMNΔ7A is not sufficient for fruit fly development, at least when expressed using the native promoter (Fig. 6C).

To examine the importance of the Slmb degron in a mammalian system, two previously developed SMA mouse models were utilized. As mentioned above, the 'Delta7' mouse (*Smn*$^{-/-}$*;SMN2;SMNΔ7*), is a model of severe SMA (Le et al. 2005), and affected pups usually die between P10 and P18 (Avg. P15). The '2B/–' mouse (*Smn*$^{2B/-}$) is a model of intermediate SMA (Bowerman et al. 2012; Rindt et al. 2015) and these animals survive much longer before dying, typically between P25 and P45 (Avg. P32). Adeno-associated virus serotype 9 (AAV9) was selected to deliver the SMN cDNA isoforms to these SMA mice, as this vector has previously been shown to enter and express in SMA-relevant tissues and can dramatically rescue the SMA phenotype when expressing the wild-type SMN cDNA (Foust et al. 2010; Passini et al. 2010; Valori et al. 2010; Dominguez et al. 2011; Glascock et al. 2012).

Delivery of AAV9-SMNΔ7A at P1 significantly extended survival in the intermediate 2B/– animals, resulting in 100% of the treated pups living beyond 100 days, similar to the results obtained with the full-length AAV9-SMN construct (Fig. 7A). In contrast, untreated 2B/– animals lived, on average, only 30 days. Mice treated with AAV9-SMNΔ7S survived an average of 45 days (Fig. 7A). Interestingly, mice treated with AAV9-SMNΔ7D, a phosphomimetic of the wild-type serine 270 residue, have an average life span that is equivalent or slightly shorter than that of untreated 2B/– mice (Fig. 7A). These results not only highlight the specificity of the S270A mutation in conferring efficacy to SMNΔ7, but also illustrate that AAV9-mediated delivery of protein alone does not improve the phenotype.

We also analyzed the effects of SMNΔ7A expression in the severe Delta7 mouse model (Le et al. 2005). Treatment with AAV9-SMNΔ7A had only a very modest effect on Delta7 mice, as none of the animals (treated or untreated) survived weaning (Fig. S2). These findings are similar to the results in *Drosophila*, upon transgenic expression of SMNΔ7A in the *Smn* null background (Fig. 6B). Thus expression of SMNΔ7A provides a clear protective benefit to the viability of intermediate mice, but not to severe SMA models.

Consistent with the lifespan data, AAV9-SMNΔ7A treated 2B/– mice gained significantly more weight than either untreated or AAV-SMNΔ7S treated animals, nearly achieving the same weight as pups treated with full-length SMN cDNA (Fig. 7B). Treatment with full-length SMN cDNA resulted in animals that were clearly stronger and more mobile, consistent with the weight data (Fig. 7C). Although they did not perform as well as mice treated with full-length SMN cDNA, the SMNΔ7A treated animals retained strength and gross motor function at late time points (e.g. P100), as measured by their ability to splay their legs and maintain a hanging position using a modified tube-test, (Fig. 7C). Animals treated with AAV9-SMNΔ7D and -SMNΔ7S did not survive long enough for testing.

Finally, to examine the functionality of SMNΔ7A in disease-relevant human tissue, control and SMA induced pluripotent stem cell (iPSC) motor neuron cultures were transduced with lentiviral vectors expressing SMNΔ7A or an mCherry control (Figs. 7D,E). At 4 weeks post-differentiation, no statistical difference was observed between control and SMA motor neurons, however by 6 weeks, SMA motor neuron numbers had

decreased significantly to approximately 7% of the total cell population (Fig. 7D). In contrast, expression of SMNΔ7A maintained motor neuron numbers to approximately the same level as the controls, and nearly two-fold greater than untreated cells (Fig. 7D). Thus expression of SMNΔ7A improves survival of human iPSCs when differentiated into motor neuron lineages.

Discussion

Factors that recognize the putative SMNΔ7-specific degron have not been identified and the molecular mechanisms governing proteasomal access to SMN and SMNΔ7 remain unclear. In this study, we isolated factors that co-purifiy with SMN from *Drosophila* embryos that exclusively express Flag-SMN. This approach reduces potential bias towards SMN partner proteins that may be more abundant in a given tissue or cell line (Charroux et al. 1999; Meister et al. 2001; Pellizzoni et al. 2002; Kroiss et al. 2008; Trinkle-Mulcahy et al. 2008; Guruharsha et al. 2011). Because the entire reading frame of fruitfly *Smn* is contained within a single exon, only full-length SMN protein is expressed in flies (Rajendra et al. 2007). Here, we identify the SCF^{Slmb} E3 ubiquitin ligase complex as a novel SMN binding partner whose interaction is conserved in human. Depletion of Slmb or B-TrCP by RNAi resulted in an increase in steady-state SMN levels in *Drosophila* and human cells, respectively. Furthermore, we detected four distinct high molecular weight SMN bands following immunoprecipitation with Flag-Slmb, likely corresponding to ubiquitylated isoforms. Finally, we showed that ectopic expression of $SMN\Delta7^{S270A}$, but not SMNΔ7 or $SMN\Delta7^{S270D}$, a phosphomimetic, is a protective modifier of SMA phenotypes in animal models and human iPSC cultures.

The SCF^{Slmb} degron is exposed by *SMN2* exon skipping

A previous study posited that a degron was specifically created by exon 7 skipping and that this event represented a key aspect of the SMA disease mechanism (Cho and Dreyfuss 2010). Our identification of a putative Slmb binding site (phospho-degron) located in the C-terminal self-oligomerization domain of SMN has allowed us to explore the molecular details of this hypothesis. The mutation of a conserved serine within the Slmb degron not only disrupted the interaction between SMN and Slmb, but also stabilized full-length SMN and SMNΔ7. Notably, the degron mutation has a greater effect

on SMN levels (both full-length and Δ7) when made in the context of a protein that does not efficiently self-oligomerize. These and other findings strongly suggest that the Slmb degron is uncovered when SMN is monomeric, whereas it is less accessible when SMN forms higher-order multimers. On the basis of these results, we conclude that *SMN2* exon skipping does not *create* a potent protein degradation signal; rather, it *exposes* an existing one.

SMN may be targeted by multiple E3 ubiquitin ligases

SMN degradation via the UPS is well-established (Chang et al. 2004; Burnett et al. 2009; Kwon et al. 2011). Accordingly, investigators have studied other E3 ligases that likely target SMN for degradation. Using a candidate approach, mind bomb 1 (Mib1) was shown to interact with and ubiquitylate SMN to facilitate its degradation in cultured human cells (Kwon et al. 2013). It is therefore likely that SMN is targeted by multiple E3 ubiquitin ligases, as this regulatory paradigm has been demonstrated for a number of proteins (e.g. p53; Jain and Barton 2010). Targeting of a single protein by multiple E3 ligases is thought to provide regulatory specificity by expressing the appropriate degradation complexes only within certain tissues, subcellular compartments or developmental timepoints. Moreover, ubiquitylation does not always result in immediate destruction of the target; differential use of ubiquitin lysine linkages or chain length can alter a protein's fate (Mukhopadhyay and Riezman 2007; Ikeda and Dikic 2008; Liu and Walters 2010).

Avenues of future exploration include the determination of the E2 proteins that partner with SCF^{Slmb} as well as the types of ubiquitin lysine chain linkages being added to SMN. These two questions are interconnected, as ubiquitin linkage specificity is determined by the E2 (Ye and Rape 2009). Lysine 48 (K48) linked chains typically result in degradation of the targeted protein by the 26S proteasome, whereas lysine 63 (K63) linkage is more commonly associated with lysosomal degradation and nonproteolytic functions such as endocytosis (Tan et al. 2007; Kirkin et al. 2009; Lim and Lim 2010). Interestingly, recent work has implicated defects in endocytosis in SMA (Custer and Androphy 2014; Dimitriadi et al. 2016; Hosseinibarkooie et al. 2016). It remains to be determined how the ubiquitylation status of SMN might intersect with endocytic functions.

In the Flag-SMN pulldown, we identified three E2 proteins as potential SMN interacting partners (Fig. 1B). Among them, Bendless (Ben) is particularly interesting because SMN co-purifies with Flag-Ben in S2 cells (Fig. S3). Ube2N, the human ortholog of Ben, heterodimerizes with Uev1a to form K63 ubiquitin linkages (Ye and Rape 2009; van Wijk and Timmers 2010; Komander and Rape 2012; Marblestone et al. 2013; Zhang et al. 2013). Bendless-Uev1a is involved in upstream activation of both JNK and IMD signaling in *Drosophila* (Paquette et al. 2010; Zhou et al. 2005). Additionally, mutations in all three components of SCF^{Slmb} lead to constitutive expression of antimicrobial peptides, which are downstream of the IMD pathway (Khush et al. 2002). Previously, we and others have shown that JNK signaling is dysregulated in animal models of SMA (Garcia et al. 2013; Genabai et al. 2015; Garcia et al. 2016; Ahmad et al. 2016). Together, these findings suggest the interesting possibility of SMN as a signaling hub linking the ubiquitin proteasome system to JNK and IMD signaling, all of which have been shown to be disrupted in SMA.

Ben has not previously been shown to function with SCF^{Slmb}, so we do not know if SMN forms a single complex with Ben (E2) and SCF^{Slmb} (E3) or if they are part of separate ubiquitylation complexes interacting independently with SMN. One established E2 partner of SCF^{Slmb} in flies is UbcD1 (Bocca et al. 2001). The human ortholog of this protein is Ube2D, and it catalyzes different types of ubiquitin linkages (Ye and Rape 2009; Komander and Rape 2012; Zhang et al. 2013). Thus, SCF^{Slmb} could operate with multiple E2s or the linkage specificity of UbcD1/Ube2D might depend on other associated adaptors. These are not mutually exclusive possibilities, so additional work will be needed in this area.

Phosphorylation of the Slmb degron within SMN

As Slmb is known to recognize phospho-degrons, one of the first questions raised by our study concerns the identity of the kinase(s) responsible for phosphorylating the degron in SMN. A prime candidate is GSK3B, as this kinase recognizes a motif (SxxxS/T; Liu et al. 2007; Lee et al. 2013) that includes the degron and extends N-terminally (^{262}SxxxSxxxSxxxT^{274}, numbering as per human SMN). In support of this hypothesis, we identified the *Drosophila* GSK3B orthologue, Shaggy (Sgg), in our SMN pulldowns (Fig. 1B). Moreover, GSK3B inhibitors as well as siRNA mediated knockdown of GSK3B were

shown to increase SMN levels, primarily by stabilizing the protein (Makhortova et al. 2011; Chen et al. 2012). Finally, GSK3B is also responsible for phosphorylation of a degron in β-catenin, a well-characterized SCF^{Slmb} substrate (Liu et al. 2002). SMA mice have low levels of UBA1 (E1) ultimately leading to accumulation of β-catenin (Wishart et al. 2014). Pharmacological inhibition of β-catenin improved neuromuscular pathology in *Drosophila*, zebrafish, and mouse SMA models. β-catenin had previously been shown to regulate motor neuron differentiation and stability primarily through affecting synaptic structure and function (Murase et al. 2002; Li et al. 2008; Ojeda et al. 2011). Beta-catenin also regulates motor neuron differentiation by retrograde signaling from skeletal muscle (Li et al. 2008). The connections of UBA1 and multiple SCF^{Slmb} substrates to motor neuron health thus places the UPS at the center of SMA research interest. All together, these findings strongly suggest that signaling cascades involving GSK3 act to regulate SMN levels in both humans and flies.

Conclusions

In summary, this study identifies conserved factors that regulate SMN stability. To our knowledge, this work represents the first time that SMN complexes have been purified in the context of an intact developing organism. Using this approach, we have demonstrated that the SCF^{Slmb} E3 ligase complex interacts with a degron embedded within the self-oligomerization domain of SMN. Our findings establish plausible connections to disease-relevant cellular processes and signaling pathways. Further, they elucidate a model whereby accessibility of the SMN phospho-degron is regulated by self-multimerization, providing an elegant mechanism for balancing functional activity with degradation.

Experimental procedures

Fly stocks and genetics

Oregon-R was used as the wild-type control allele. The *Smn*^{X7} microdeletion allele (Chang et al. 2008) was a gift from S. Artavanis-Tsakonis (Harvard University, Cambridge, USA). This deficiency removes the promoter and the entire SMN coding region, leaving only the final 44bp of the 3' UTR. All stocks were cultured on molasses and agar at room temperature (24 ± 1°C) in half-pint bottles. The WT transgene construct was injected into embryos by BestGene Inc. (Chino Hills, CA).

SMN constructs

A ~3kb fragment containing the entire *Smn* coding region was cloned from the *Drosophila* genome into the pAttB vector (Bischof et al. 2007). A 3X FLAG tag was inserted immediately downstream of the start codon of dSMN. Point mutations were introduced into this construct using Quickchange (Invitrogen) site-directed mutagenesis according to manufacturer's instructions. The transgenes were injected directly into embryos heterozygous for the *Smn*^{X7} microdeletion (Chang et al. 2008) that was recombined prior to injection with the 86F8 PhiC31 landing site (Bloomington Stock Center, IN, USA).

Drosophila embryo protein lysate and mass spectrometry

0-12h Drosophila embryos were collected from Oregon-R control and Flag-SMN flies, dechorionated, flash frozen, and stored at -80C. Embryos (approx. 1gr) were then homogenized on ice with a Potter tissue grinder in 5 mL of lysis buffer containing 100mM potassium acetate, 30mM HEPES-KOH at pH 7.4, 2mM magnesium acetate, 5mM dithiothreitol (DTT) and protease inhibitor cocktail. Lysates were centrifuged twice at 20000 rpm for 20min at 4C and dialyzed for 5h at 4C in Buffer D (HEPES 20mM pH 7.9, 100mM KCl, 2.5 mM $MgCl_2$, 20% glycerol, 0.5 mM DTT, PMSF 0.2 mM). Lysates were clarified again by centrifugation at 20000 rpm for 20 min at 4C. Lysates were flash frozen using liquid nitrogen and stored at -80C before use. Lysates were then thawed on ice, centrifuged at 20000 rpm for 20 min at 4C and incubated with rotation with 100 μL of EZview Red Anti-FLAG M2 affinity gel (Sigma) for 2h at 4C. Beads were washed a total of six times using buffer with KCl concentrations ranging from 100mM to 250mM with rotation for 1 min at 4C in between each wash. Finally, Flag proteins were eluted 3

consecutive times with one bed volume of elution buffer (Tris 20mM pH 8, 100 mM KCl, 10% glycerol, 0.5 mM DTT, PMSF 0.2 mM) containing 250ug/mL 3XFLAG peptide (sigma). The entire eluate was used for mass spectrometry analysis on an Orbitrap Velos instrument, fitted with a Thermo Easy-spray 50cm column.

Tissue culture and transfections

S2 cell lines were obtained from the Drosophila Genome Resource Center (Bloomington, IL). S2 cells were maintained in SF900 SFM (Gibco) supplemented with 1% penicillin/streptomycin and filter sterilized. Cells were removed from the flask using a cell scraper and passaged to maintain a density of approximately 10^6-10^7 cells/mL. S2 cells were transferred to filter sterilized SF900 SFM (Gibco) without antibiotics prior to transfection with Cellfectin II (Invitrogen). Transfections were performed according to Cellfectin II protocol in a final volume of 4 mL in a T-25 flask containing 10^7 cells that were plated one hour before transfection. The total amount of DNA used in transfections was 2.5ug. Human embryonic kidney HEK-293T and HeLa cells were maintained at 37C with 5% CO_2 in DMEM (Gibco) supplemented with 10% FBS and 1% penicillin/streptomycin (Gibco). $1x10^6$ - $2x10^6$ cells were plated in T-25 flasks and transiently transfected with 1-2ug of plasmid DNA per flask using Lipofectamine (Invitrogen) or FuGENE HD transfection reagent (Roche Applied Science, Indianapolis, IN) according to the manufacturer's protocol. Cells were harvested 24-72 h posttransfection.

For siRNA transections, HeLa cells were plated subconfluently in T-25 flasks and transfected with 10nm of siRNA (Gift from Mike Emanuele lab) and 17uL Lipofectamine RNAi MAX (Invitrogen) in 5mL total media according to manufacturers instructions. After 48h of transfection cells were harvested. For RNAi in S2 cells using dsRNA, 10^7 cells were plated in each well of a 6-well plate in 1 mL of media. Cells were treated ~ every 24h with 10ug/mL dsRNA targeted against Slmb or Oskar as a control as described in Rogers and Rogers 2008.

Cycloheximide Treatment

Following RNAi treatment, S2 cells were pooled, centrifuged and resuspended in fresh media. 1/3 of these cells were frozen and taken as the 0h timepoint. The remainders of

the cells were replated in 6 well plates. 100ug/mL cycloheximide (CHX) was added to each sample, and cells were harvested at 2 and 6 hours following treatment.

Immunoprecipitation

Clarified cell lysates were precleared with immune-globulin G (IgG) agarose beads for 1h at 4C and again precleared overnight at 4C. The precleared lysates were then incubated with Anti-FLAG antibody crosslinked to agarose beads (EZview Red Anti-FLAG M2 affinity gel, Sigma) for 2h at 4C with rotation. The beads were washed with lysis buffer or modified lysis buffer six times and boiled in SDS gel-loading buffer. Eluted proteins were run on an SDS-PAGE for western blotting.

Antibodies and Western blotting

Larval and adult lysates were prepared by crushing the animals in lysis buffer (50mM Tris-HCl, pH 7.5, 150 mM NaCl, 1mM EDTA, 1% NP-40) with 1X (adults) or 10x (larvae) protease inhibitor cocktail (Invitrogen) and clearing the lysate by centrifugation at 13,000 RPM for 10 min at 4ºC. S2 cell lysates were prepared by suspending cells in lysis buffer (50mM Tris-HCl, pH 7.5, 150 mM NaCl, 1mM EDTA, 1% NP-40) with 10% glycerol and 1x protease inhibitor cocktail (Invitrogen) and disrupting cell membranes by pulling the suspension through a 25 gauge needle (Becton Dickinson). The lysate was then cleared by centrifugation at 13,000 RPM for 10 min at 4ºC. Human cells (293Ts and HeLas) were first gently washed in ice-cold 1X PBS, then collected in ice-cold 1X PBS by scraping. Cells were pelleted by spinning at 1000 rpm for 5 min. The supernatant was removed and cells were resuspended in ice cold lysis buffer (50mM Tris-HCl, pH 7.5, 150 mM NaCl, 1mM EDTA, 1% NP-40) and allowed to lyse on ice for 30 min. After lysing, the lysate was cleared by centrifuging the cells for 10 min at 13000 at 4C. Western blotting on lysates was performed using standard protocols. Rabbit anti-dSMN serum was generated by injecting rabbits with purified full-length dSMN protein (Pacific Immunology Corp, CA), and was subsequently affinity purified. For Western blotting, dilutions of 1 in 2,500 for the affinity purified anti-dSMN, 1 in 20,000 (fly) or 1 in 5,000 (human) for anti-α tubulin (Sigma), 1 in 10,000 for monoclonal anti-Flag (Sigma), 1 in 1,000 for anti-Slmb (gift from Greg Rogers), 1 in 2,500 for anti-human SMN (BD Biosciences), 1 in 1,000 for anti-B-TrCP (gift from MB Major lab), and 1 in 10,000 for polyclonal anti-Myc (Santa Cruz) were used.

Human iPSC Cell culture

Human iPSCs from two independent unaffected control and two SMA patient lines were grown as pluripotent colonies on Matrigel substrate (Corning) in Nutristem medium (Stemgent). Colonies were then lifted using 1mg/ml Dispase (Gibco) and maintained as floating spheres of neural progenitor cells in the neural progenitor growth medium Stemline (Sigma) supplemented with 100ng/ml human basic fibroblast growth factor (FGF-2, Miltenyi), 100ng/ml epidermal growth factor (EGF, Miltenyi), and 5μg/ml heparin (Sigma-Aldrich) in ultra-low attachment flasks. Aggregates were passaged using a manual chopping technique as previously described (Svendsen et al. 1998; Ebert et al. 2013). To induce motor neuron differentiation, neural progenitor cells were cultured in neural induction medium (1:1 DMEM/F12 (Gibco), 1x N2 Supplement (Gibco), 5μg/mL Heparin (Sigma), 1x Non-Essential Amino Acids (Gibco), and 1x Antibiotic-Antimycotic (Gibco)) plus 0.1μM all-trans retinoic acid (RA) for two weeks; 1μM Purmorphamine (PMN, Stemgent) was added during the second week. Spheres were then dissociated with TrypLE Express (Gibco) and plated onto Matrigel-coated 12mm coverslips in NIM plus 1μM RA, 1μM PMN, 1x B27 Supplement (Gibco), 200ng/mL Ascorbic Acid (Sigma), 1μM cAMP (Sigma), 10ng/mL BDNF (Peprotech), 10ng/mL GDNF (Peprotech)). One week post-plating, cells were infected with lentiviral vectors (MOI = 5) expressing mCherry alone or SMN S270A-IRES-mCherry. Transgenes in both viruses were under the control of the EF1α promoter. Uninfected cells served as controls. Cells were analyzed at 1 and 3 weeks post-infections, which was 4 and 6 weeks of total differentiation (Ebert et al. 2009; Sareen et al. 2013).

Immunocytochemistry

Coverslips were fixed in 4% paraformaldehyde (Electron Microscopy Sciences) for 20 minutes at room temperature and rinsed with PBS. Cells were blocked with 5% Normal Donkey Serum (Millipore) and permeabilized in 0.2% TritonX-100 (Sigma) for 30 minutes at room temperature. Cells were then incubated in primary antibody solution for 1 hour, rinsed with PBS, and incubated in secondary antibody solution for 1 hour at room temperature. Finally, nuclei were labeled with Hoechst nuclear stain (Sigma) to label DNA and mounted onto glass slides using FluoroMount medium (SouthernBiotech). Primary antibodies used were mouse anti-SMI-32 (Covance SMI-32R, 1:1000) and rabbit anti-mCherry (ThermoFisher, 1:1000). Secondary antibodies used were donkey

anti-rabbit Cy3 (Jackson Immunoresearch 711-165-152) and donkey anti-mouse AF488 (Invitrogen A21202).

Immunocytochemical Analysis

Images were acquired from five random fields per coverslip using an inverted fluorescent microscope (Nikon) and NIS Elements software. Images were blinded and manually analyzed for antigen specificity with NIS Elements software.

Acknowledgements

This work was supported by NIGMS R01 GM118636 (to A.G.M.). K.M.G. was supported by graduate research fellowship DGE-1144081 from the NSF. Work in the Wagner lab (D.B and E.J.W.) was supported by the Welch Foundation (H1889). We also thank the Peifer, Emanuele, Major, and Rogers laboratories for reagents, advice and expertise.

Figure Legends

Figure 1: Flag-SMN immunopurified lysates contain known protein interaction partners and ubiquitin proteasome system (UPS) proteins ***A.*** Protein lysates from control Oregon-R Drosophila melanogaster embryos and embryos expressing only transgenic Flag-SMN were Flag-immunopurified and proteins were separated by gel electrophoresis. Flag-SMN was identified, along with other core SMN complex components such as the Sm proteins and the Gemins as being enriched compared to the control sample. ***B***. Flag-purified embryonic lysates were analyzed by 'label-free' mass spectrometry. Numerous proteins interacting with Flag-SMN are involved in the ubiquitin proteasome system (UPS). Of these UPS proteins, Cullin 1, SkpA, and supernumerary limbs (Slmb), were highly enriched (at least 10 fold) in Flag-SMN samples as compared to the control sample. ***C.*** Slmb-SMN interaction in the embryonic lysates was verified using Slmb antibody. Slmb was abundant in Flag immunopurified eluate from flies expressing Flag-SMN, while background levels were nearly undetectable in purified eluate from control flies.

Figure 2. Conserved interaction between SMN and the $SCF^{Slmb/B\text{-}TrCP}$ E3 ubiquitin ligase. ***A***. The interactions of Roc1a, Cullin1, SkpA, and Slmb were verified in a co-immunoprecipitation demonstrating Flag-tagged SCF components interact with Myc-SMN in Drosophila S2 cells. SMN was detected at high levels following immunoprecipitation of Cul1-Flag and Flag-Slmb. SMN was also detected above background following immunoprecipitation of Flag-Roc1a and SkpA-Flag. ***B***. Following Flag-Slmb immunoprecipitation, western analysis using anti-SMN antibody for endogenous SMN was carried out. A protein ladder, with each band separated by ~8kDa, was detected. Notably, this ladder is not visible following immunoprecipitation of Cul1 (shown) or any other SCF^{Slmb} component or Gemin2 (not shown). ***C.*** The interaction of Flag-tagged Drosophila SCF components with endogenous human SMN was tested in in HEK 293T cells. Human SMN was detected at high levels following immunoprecipitation of Drosophila Flag-Cul1 and Flag-Slmb and detected at a lower level following Drosophila Flag-SkpA immunoprecipitation. ***D.*** Flag-tagged versions of the human homologs of Slmb, Flag-B-TrCP1 and Flag-B-TrCP2, interact with endogenous human SMN in HEK 293T cells demonstrated by Flag-immunopurification followed by immunodetection of SMN.

Figure 3. Depletion of Slmb/B-TrCP results in modest increase of SMN levels ***A.*** Depletion of Slmb using dsRNA in Drosophila S2 cells resulted in modestly increased SMN levels. Following Slmb RNAi, full-length SMN levels were slightly increased as compared to cells treated with control dsRNA against Oskar, which is not expressed in S2 cells. ***B.*** The effect of B-TrCP depletion on SMN levels in human cells was tested using siRNA that targets both B-TrCP1 and B-TrCP2 in HeLa cells. We detected a modest increase in levels of full-length endogenous SMN after B-TrCP RNAi but not control (scramble) RNAi. ***C***. Drosophila S2 cells were treated with cycloheximide (CHX), an inhibitor of protein synthesis, following Slmb depletion using dsRNA to test whether differences in protein levels would be exacerbated when the production of new protein was prevented. Protein was collected at 0, 2, and 6 hours post CHX treatment. At 6 hours post-CHX treatment there is a modest increase in full-length SMN levels following Slmb RNAi as compared to the initial timepoint (0h) and as compared to control (Oskar) RNAi treatment.

Figure 4: Identification and mutation of a putative Slmb/B-TrCP phospho-degron ***A***. Identification of a conserved putative Slmb phospho-degron (DpSGXXpS/T motif variant) in the C-terminal self-oligomerization domain (YG Box) of SMN. To generate a more vertebrate-like SMN, key amino acids in Drosophila SMN were changed to amino acids conserved in vertebrates. Using this SMN backbone, a serine to alanine mutation was made in the putative degron in both full-length (vSMNS201A) and truncated SMNΔ7 (vSMNΔ7A). An additional SMN construct that is the same length as SMNΔ7, but has the amino acid sequence GLRQ (the next amino acids in the sequence) rather than EMLA (the amino acids introduced by mis-splicing of *SMN2*) was made. The same serine to alanine mutation was made in this construct as well (MGLRQ* and MGLRQ*S201A). ***B.*** Western blotting was used to determine protein levels of each of these SMN constructs, with expression driven by the endogenous promoter, in Drosophila S2 cells. Each of these SMN constructs (vSMN, vSMNΔ7S, and MGLRQ*) shows increased protein levels when the serine is mutated to an alanine, indicating disruption of the normal degradation of SMN. Additionally, MGLRQ* protein is present at higher levels than is vSMNΔ7S. Normalized fold change as compared to vSmn levels is indicated at the bottom. ***C.*** Flag-tagged SMN constructs were co-transfected with Myc-Slmb in Drosophila S2 cells. Protein lysates were Flag-immunoprecipitated and probed with anti-Myc antibody to detect SMN-Slmb interaction. In both full-length SMN (vSMN)

and truncated SMN (vSMNΔ7), serine to alanine mutation decreased interaction of Slmb with SMN. Truncated SMN (vSMNΔ7) showed a dramatically increased interaction with Slmb as compared to full-length SMN (vSMN).

Figure 5: SMN self-oligomerization regulates access to Slmb phospho-degron ***A***. Full-length SMN constructs containing point mutations known to decrease self-oligomerization (Y203C and G206S) and a mutation that does not disrupt self-oligomerization in the fly (G210V) with and without the serine to alanine mutation were transfected in Drosophila S2 cells. The serine to alanine mutation has an increased stabilizing effect when made in SMN with poor self-oligomerization capability. ***B.*** Graph showing normalized quantification of SMN protein levels.

Figure 6: Low levels of SMNΔ7A are insufficient to improve viability in fruit fly models of SMA ***A***. vSmn and vSmnS201A transgenes produce fully viable and fertile adults. The eclosion frequencies of these animals (83% and 97.5% respectively) is higher than that of flies expressing wild-type Flag-Smn (67%). ***B.*** Neither Flag-vSmnΔ7S nor -vSmnΔ7A was able to rescue viability of the *Smn* null allele; these animals also died as late 2nd or early 3rd instar larvae. Furthermore, when crossed to other allelic combinations, V72G (intermediate) and WT (mild), the constructs did not provide a protective benefit. ***C.*** Western blot showing protein levels of full length Flag-Smn in each of the fly lines depicted in Part B. vSMNΔ7A protein is not sufficient for fruit fly development, at least when expressed at relatively low levels from the native *Smn* promoter.

Figure 7: SMNΔ7A is a modifier of the SMA phenotype in mouse models and human cell culture models of SMA ***A***. Delivery of AAV9-SMNΔ7A at P1 significantly extended survival in the intermediate 2B/– animals, resulting in 100% of the treated pups living beyond 100 days, similar to the results obtained with the full-length AAV9-SMN construct. Untreated 2B/– animals lived, on average, only 30 days. Mice treated with AAV9-SMNΔ7S survived an average of 45 days. Mice treated with AAV9 expressing SMNΔ7D (phosphomimetic) have an average life span that is equivalent or slightly worse than that of untreated 2B/– mice. ***B.*** AAV9-SMNΔ7A treated mice also gained significantly more weight than either untreated or AAV-SMNΔ7S treated animals, nearly achieving the same weight as 2B/– pups treated with full-length SMN cDNA. ***C.*** AAV-SMNΔ7A treated animals retained their improved strength and gross motor functions at late time points (P100), as measured by their ability to splay their legs and maintain a hanging position using a modified tube-test. Treatment with full-length SMN cDNA

resulted in animals that were significantly stronger and more mobile, consistent with the weight data. ***D.*** At 4 weeks post-differentiation, no statistical difference was observed between control and SMA motor neurons. At 6 weeks, SMA motor neuron numbers had decreased significantly to approximately 7% of the total cell population. Expression of SMNΔ7A maintained motor neuron numbers to approximately the same level as the controls, and nearly two-fold greater than untreated cells. ***D.*** Control and SMA Induced pluripotent stem cell (iPSC) motor neuron cultures were transduced with lentiviral vectors expressing SMNΔ7A or an mCherry control.

Figure S1: Levels of vSmnΔ7A in flies with one copy of the transgene and a balancer chromosome were relatively low. The vSmnΔ7S transgene was barely detectable in comparison to the full-length constructs (vSmn and vSmn^{S201A}).

Figure S2: Survival analysis of the effects of SMNΔ7A expression in the severe Delta7 mouse model. Treatment with AAV9-SMNΔ7A had only a very modest effect on viability and none of the animals survived weaning.

Figure S3: The interaction of SMN with Bendless (Ben) was verified in a co-immunoprecipitation demonstrating Flag-tagged Ben interacts with Myc-SMN in Drosophila S2 cells. SMN interaction with Flag-Slmb was used as a positive control for protein interaction.

References

Ackermann B, Kröber S, Torres-Benito L, Borgmann A, Peters M, Hosseini Barkooie SM, Tejero R, Jakubik M, Schreml J, Milbradt J, et al. 2013. Plastin 3 ameliorates spinal muscular atrophy via delayed axon pruning and improves neuromuscular junction functionality. *Hum Mol Genet* **22**: 1328–1347.

Ahmad S, Bhatia K, Kannan A, Gangwani L. 2016. Molecular Mechanisms of Neurodegeneration in Spinal Muscular Atrophy. *J Exp Neurosci* **10**: 39–49.

Bischof J, Maeda RK, Hediger M, Karch F, Basler K. 2007. An optimized transgenesis system for Drosophila using germ-line-specific phiC31 integrases. *Proc Natl Acad Sci U S A* **104**: 3312–3317.

Bocca SN, Muzzopappa M, Silberstein S, Wappner P. 2001. Occurrence of a putative SCF ubiquitin ligase complex in Drosophila. *Biochem Biophys Res Commun* **286**: 357–364.

Bowerman M, Anderson CL, Beauvais A, Boyl PP, Witke W, Kothary R. 2009. SMN, profilin IIa and plastin 3: A link between the deregulation of actin dynamics and SMA pathogenesis. *Mol Cell Neurosci* **42**: 66–74.

Bowerman M, Murray LM, Beauvais A, Pinheiro B, Kothary R. 2012. A critical smn threshold in mice dictates onset of an intermediate spinal muscular atrophy phenotype associated with a distinct neuromuscular junction pathology. *Neuromuscul Disord* **22**: 263–276.

Burghes Arthur HM, Beattie Christine E. 2009. Spinal muscular atrophy: why do low levels of survival motor neuron protein make motor neurons sick? *Nat Rev Neurosci* **10**: 597–609.

Burnett BG, Muñoz E, Tandon A, Kwon DY, Sumner CJ, Fischbeck KH. 2009. Regulation of SMN protein stability. *Mol Cell Biol* **29**: 1107–1115.

Cauchi RJ, Sanchez-Pulido L, Liu J-L. 2010. Drosophila SMN complex proteins Gemin2, Gemin3, and Gemin5 are components of U bodies. *Exp Cell Res* **316**: 2354–2364.

Chan YB. 2003. Neuromuscular defects in a Drosophila survival motor neuron gene mutant. *Hum Mol Genet* **12**: 1367–1376.

Chang HCH, Dimlich DN, Yokokura T, Mukherjee A, Kankel MW, Sen A, Sridhar V, Fulga TA, Hart AC, Van Vactor D, et al. 2008. Modeling spinal muscular atrophy in Drosophila. *PLoS One* **3**: e3209.

Chang HC, Hung WC, Chuang YJ, Jong YJ. 2004. Degradation of survival motor neuron (SMN) protein is mediated via the ubiquitin/proteasome pathway. *Neurochem Int* **45**: 1107–1112.

Charroux B, Pellizzoni L, Perkinson RA, Shevchenko A, Mann M, Dreyfuss G. 1999. Gemin3: A novel DEAD box protein that interacts with SMN, the spinal muscular atrophy gene product, and is a component of gems. *J Cell Biol* **147**: 1181–1193.

Chen PC, Gaisina IN, El-Khodor BF, Ramboz S, Makhortova NR, Rubin LL, Kozikowski AP. 2012. Identification of a maleimide-based glycogen synthase kinase-3 (GSK-3) inhibitor, BIP-135, that prolongs the median survival time of Δ7 SMA KO mouse model of spinal muscular atrophy. *ACS Chem Neurosci* **3**: 5–11.

Cho S, Dreyfuss G. 2010. A degron created by SMN2 exon 7 skipping is a principal contributor to spinal muscular atrophy severity. *Genes Dev* **24**: 438–442.

Coovert DD, Le TT, McAndrew PE, Strasswimmer J, Crawford TO, Mendell JR, Coulson SE, Androphy EJ, Prior TW, Burghes AHM. 1997. The survival motor neuron protein in spinal muscular atrophy. *Hum Mol Genet* **6**: 1205–1214.

Crawford TO, Pardo CA. 1996. The Neurobiology of Childhood Spinal Muscular Atrophy. *Neurobiol Dis* **3**: 97–110.

Custer SK, Androphy EJ. 2014. Autophagy dysregulation in cell culture and animals models of spinal muscular atrophy. *Mol Cell Neurosci* **61**: 133–140.

Dimitriadi M, Derdowski A, Kalloo G, Maginnis MS, Bliska B, Sorkaç A, Q Nguyen KC, Cook SJ, Poulogiannis G, Atwood WJ, et al. 2016. Decreased function of survival motor neuron protein impairs endocytic pathways. *Proc Natl Acad Sci U S A* 4377–4386.

Dominguez E, Marais T, Chatauret N, Benkhelifa-Ziyyat S, Duque S, Ravassard P, Carcenac R, Astord S, de Moura AP, Voit T, et al. 2011. Intravenous scAAV9 delivery of a codon-optimized SMN1 sequence rescues SMA mice. *Hum Mol Genet* **20**: 681–693.

Ebert AD, Yu J, Rose FF, Mattis VB, Lorson CL, Thomson JA, Svendsen CN. 2009. Induced pluripotent stem cells from a spinal muscular atrophy patient. *Nature* **457**: 277–280.

Ebert AD, Shelley BC, Hurley AM, Onorati M, Castiglioni V, Patitucci TN, Svendsen SP, Mattis VB, McGivern J V., Schwab AJ, et al. 2013. EZ spheres: A stable and expandable culture system for the generation of pre-rosette multipotent stem cells from human ESCs and iPSCs. *Stem Cell Res* **10**: 417–427.

Fan L, Simard LR. 2002. Survival motor neuron (SMN) protein: role in neurite outgrowth and neuromuscular maturation during neuronal differentiation and development. *Hum Mol Genet* **11**: 1605–1614.

Fischer U, Liu Q, Dreyfuss G. 1997. The SMN-SIP1 Complex Has an Essential Role in Spliceosomal snRNP Biogenesis. *Cell* **90**: 1023–1029.

Foust KD, Wang X, McGovern VL, Braun L, Bevan AK, Haidet AM, Le TT, Morales PR, Rich MM, Burghes AHM, et al. 2010. Rescue of the spinal muscular atrophy phenotype in a mouse model by early postnatal delivery of SMN. *Nat Biotechnol* **28**: 271–274.

Frescas D, Pagano M. 2008. Deregulated proteolysis by the F-box proteins SKP2 and B-TrCP: tipping the scales of cancer. *Nat Rev Cancer* **8**: 438–449.

Fuchs SY, Spiegelman VS, Kumar KGS. 2004. The many faces of B-TrCP E3 ubiquitin ligases: reflections in the magic mirror of cancer. *Oncogene* **23**: 2028–2036.

Garcia EL, Lu Z, Meers MP, Praveen K, Matera AG. 2013. Developmental arrest of Drosophila survival motor neuron (Smn) mutants accounts for differences in expression of minor intron-containing genes. *RNA* **19**: 1510–1516.

Garcia EL, Wen Y, Praveen K, Matera AG. 2016. Transcriptomic comparison of Drosophila snRNP biogenesis mutants reveals mutant-specific changes in pre-mRNA processing: implications for spinal muscular atrophy. *RNA* 1–13.

Gates J, Lam G, Ortiz J, Losson R, Thummel CS. 2004. rigor mortis encodes a novel nuclear receptor interacting protein required for ecdysone signaling during Drosophila larval development. *Development* **131**: 25–36.

Genabai NK, Ahmad S, Zhang Z, Jiang X, Gabaldon CA, Gangwani L. 2015. Genetic inhibition of JNK3 ameliorates spinal muscular atrophy. *Hum Mol Genet* **24**: 6986–7004.

Glascock JJ, Shababi M, Wetz MJ, Krogman MM, Lorson CL. 2012. Direct central nervous system delivery provides enhanced protection following vector mediated gene replacement in a severe model of Spinal Muscular Atrophy. *Biochem Biophys Res Commun* **417**: 376–381.

Groen EJN, Gillingwater TH. 2015. UBA1: At the Crossroads of Ubiquitin Homeostasis and Neurodegeneration. *Trends Mol Med* **21**: 622–632.

Gupta K, Martin R, Sharp R, Sarachan KL, Ninan NS, Van Duyne GD. 2015. Oligomeric Properties of Survival Motor Neuron.Gemin2 Complexes. *J Biol Chem* **290**: 20185–20199.

Guruharsha KG, Rual J-F, Zhai B, Mintseris J, Vaidya P, Vaidya N, Beekman C, Wong C, Rhee DY, Cenaj O, et al. 2011. A protein complex network of Drosophila melanogaster. *Cell* **147**: 690–703.

Hosseinibarkooie S, Peters M, Torres-Benito L, Rastetter RH, Hupperich K, Hoffmann A, Mendoza-Ferreira N, Kaczmarek A, Janzen E, Milbradt J, et al. 2016. The Power of Human Protective Modifiers: PLS3 and CORO1C Unravel Impaired Endocytosis in Spinal Muscular Atrophy and Rescue SMA Phenotype. *Am J Hum Genet* **99**: 647–665.

Hsieh-Li HM, Chang JG, Jong YJ, Wu MH, Wang NM, Tsai CH, Li H. 2000. A mouse model for spinal muscular atrophy. *Nat Genet* **24**: 66–70.

Hsu SH, Lai MC, Er TK, Yang SN, Hung CH, Tsai HH, Lin YC, Chang JG, Lo YC, Jong YJ. 2010. Ubiquitin carboxyl-terminal hydrolase L1 (UCHL1) regulates the level of SMN expression through ubiquitination in primary spinal muscular atrophy fibroblasts. *Clin Chim Acta* **411**: 1920–1928.

Ikeda F, Dikic I. 2008. Atypical ubiquitin chains: new molecular signals. "Protein Modifications: Beyond the Usual Suspects" review series. *EMBO Rep* **9**: 536–542.

Jain AK, Barton MC. 2010. Making sense of ubiquitin ligases that regulate p53. *Cancer Biol Ther* **10**: 665–672.

Jiang J, Struhl G. 1998. Regulation of the Hedgehog and Wingless signalling pathways by the F-box/WD40-repeat protein Slimb. *Nature* **391**: 493–496.

Jin J, Ang XL, Shirogane T, Wade Harper J. 2005. Identification of substrates for F-box proteins. *Methods Enzymol* **399**: 287–309.

Kariya S, Park GH, Maeno-Hikichi Y, Leykekhman O, Lutz C, Arkovitz MS, Landmesser LT, Monani UR. 2008. Reduced SMN protein impairs maturation of the neuromuscular junctions in mouse models of spinal muscular atrophy. *Hum Mol Genet* **17**: 2552–2569.

Khush RS, Cornwell WD, Uram JN, Lemaitre B. 2002. A ubiquitin-proteasome pathway represses the Drosophila immune deficiency signaling cascade. *Curr Biol* **12**: 1728–1737.

Kim TY, Siesser PF, Rossman KL, Goldfarb D, Mackinnon K, Yan F, Yi X, MacCoss MJ, Moon RT, Der CJ, et al. 2015. Substrate trapping proteomics reveals targets of the βTrCP2/FBXW11 ubiquitin ligase. *Mol Cell Biol* **35**: 167–181.

Kirkin V, McEwan DG, Novak I, Dikic I. 2009. A Role for Ubiquitin in Selective Autophagy. *Mol Cell* **34**: 259–269.

Kolb SJ, Kissel JT. 2015. Spinal Muscular Atrophy. *Neurol Clin* **33**: 831–846.

Komander D, Rape M. 2012. The Ubiquitin Code. *Annu Rev Biochem* **81**: 203–229.

Kong L, Wang X, Choe DW, Polley M, Burnett BG, Bosch-Marce M, Griffin JW, Rich MM, Sumner CJ. 2009. Impaired Synaptic Vesicle Release and Immaturity of Neuromuscular Junctions in Spinal Muscular Atrophy Mice. *J Neurosci* **29**: 842–851.

Korhonen L, Lindholm D. 2004. The ubiquitin proteasome system in synaptic and axonal degeneration: a new twist to an old cycle. *J Cell Biol* **165**: 27–30.

Kroiss M, Schultz J, Wiesner J, Chari A, Sickmann A, Fischer U. 2008. Evolution of an RNP assembly system: a minimal SMN complex facilitates formation of UsnRNPs in Drosophila melanogaster. *Proc Natl Acad Sci U S A* **105**: 10045–10050.

Kwon DY, Dimitriadi M, Terzic B, Cable C, Hart AC, Chitnis A, Fischbeck KH, Burnett BG. 2013. The E3 ubiquitin ligase mind bomb 1 ubiquitinates and promotes the degradation of survival of motor neuron protein. *Mol Biol Cell* **24**: 1863–1871.

Kwon DY, Motley WW, Fischbeck KH, Burnett BG. 2011. Increasing expression and decreasing degradation of SMN ameliorate the spinal muscular atrophy phenotype in mice. *Hum Mol Genet* **20**: 3667–3677.

Le TT, Pham LT, Butchbach MER, Zhang HL, Monani UR, Coovert DD, Gavrilina TO, Xing L, Bassell GJ, Burghes AHM. 2005. SMNΔ7, the major product of the centromeric survival motor neuron (SMN2) gene, extends survival in mice with spinal muscular atrophy and associates with full-length SMN. *Hum Mol Genet* **14**: 845–857.

Lee YC, Liao PC, Liou YC, Hsiao M, Huang CY, Lu PJ. 2013. Glycogen synthase kinase 3 β activity is required for hBora/Aurora A-mediated mitotic entry. *Cell Cycle* **12**: 953–960.

Lefebvre S, Bürglen L, Reboullet S, Clermont O, Burlet P, Viollet L, Benichou B, Cruaud C, Millasseau P, Zeviani M, et al. 1995. Identification and characterization of a spinal muscular atrophy-determining gene. *Cell* **80**: 155–165.

Lefebvre S, Burlet P, Liu Q, Bertrandy S, Clermont O, Munnich A, Dreyfuss G, Melki J. 1997. Correlation between severity and SMN protein level in spinal muscular atrophy. *Nat Genet* **16**: 265–269.

Li DK, Tisdale S, Lotti F, Pellizzoni L. 2014. SMN control of RNP assembly: from post-transcriptional gene regulation to motor neuron disease. *Semin Cell Dev Biol*.

Li XM, Dong XP, Luo SW, Zhang B, Lee DH, Ting AKL, Neiswender H, Kim CH, Carpenter-Hyland E, Gao TM, et al. 2008. Retrograde regulation of motoneuron differentiation by muscle beta-catenin. *Nat Neurosci* **11**: 262–268.

Lim KL, Lim GGY. 2011. K63-linked ubiquitination and neurodegeneration. *Neurobiol Dis* **43**: 9–16.

Liu C, Li Y, Semenov M, Han C, Baeg GH, Tan Y, Zhang Z, Lin X, He X. 2002. Control of B-catenin phosphorylation/degradation by a dual-kinase mechanism. *Cell* **108**: 837–847.

Liu F, Walters KJ. 2010. Multitasking with ubiquitin through multivalent interactions. *Trends Biochem Sci* **35**: 352–360.

Liu M, Tu X, Ferrari-Amorotti G, Calabretta B, Baserga R. 2007. Downregulation of the upstream binding factor1 by glycogen synthase kinase3B in myeloid cells induced to differentiate. *J Cell Biochem* **100**: 1154–1169.

Lorson CL, Rindt H, Shababi M. 2010. Spinal muscular atrophy: mechanisms and therapeutic strategies. *Hum Mol Genet* **19**: R111–R118.

Lorson CL, Androphy EJ. 2000. An exonic enhancer is required for inclusion of an essential exon in the SMA-determining gene SMN. *Hum Mol Genet* **9**: 259–265.

Lorson CL, Hahnen E, Androphy EJ, Wirth B. 1999. A single nucleotide in the SMN gene regulates splicing and is responsible for spinal muscular atrophy. *Proc Natl Acad Sci U S A* **96**: 6307–6311.

Makhortova NR, Hayhurst M, Cerqueira A, Sinor-Anderson AD, Zhao WN, Heiser PW, Arvanites AC, Davidow LS, Waldon ZO, Steen JA, et al. 2011. A screen for regulators of survival of motor neuron protein levels. *Nat Chem Biol* **7**: 544–552.

Marblestone JG, Butt S, McKelvey DM, Sterner DE, Mattern MR, Nicholson B, Eddins MJ. 2013. Comprehensive Ubiquitin E2 Profiling of Ten Ubiquitin E3 Ligases. *Cell Biochem Biophys* **67**: 161–167.

Martin R, Gupta K, Ninan NS, Perry K, Van Duyne GD. 2012. The Survival Motor Neuron Protein Forms Soluble Glycine Zipper Oligomers. *Structure* **20**: 1929–1939.

Matera AG, Wang Z. 2014. A day in the life of the spliceosome. *Nat Rev Mol Cell Biol* **15**: 108–121.

McWhorter ML, Monani UR, Burghes AHM, Beattie CE. 2003. Knockdown of the survival motor neuron (Smn) protein in zebrafish causes defects in motor axon outgrowth and pathfinding. *J Cell Biol* **162**: 919–931.

Meister G, Bühler D, Pillai R, Lottspeich F, Fischer U. 2001. A multiprotein complex mediates the ATP-dependent assembly of spliceosomal U snRNPs. *Nat Cell Biol* **3**: 1–8.

Monani UR, Sendtner M, Coovert DD, Parsons DW, Andreassi C, Le TT, Jablonka S, Schrank B, Rossoll W, Prior TW, et al. 2000. The human centromeric survival motor neuron gene (SMN2) rescues embryonic lethality in Smn(-/-) mice and results in a mouse with spinal muscular atrophy. *Hum Mol Genet* **9**: 333–339.

Monani UR. 2005. Spinal Muscular Atrophy: A Deficiency in a Ubiquitous Protein; a Motor Neuron-Specif Disease. *Neuron* **48**: 885–895.

Monani UR, Lorson CL, Parsons DW, Prior TW, Androphy EJ, Burghes AHM, McPherson JD. 1999. A single nucleotide difference that alters splicing patterns distinguishes the SMA gene SMN1 from the copy gene SMN2. *Hum Mol Genet* **8**: 1177–1183.

Mukhopadhyay D, Riezman H. 2007. Proteasome-independent functions of ubiquitin in endocytosis and signaling. *Science* **315**: 201–205.

Murase S, Mosser E, Schuman EM. 2002. Depolarization drives β-catenin into neuronal spines promoting changes in synaptic structure and function. *Neuron* **35**: 91–105.

Ning K, Drepper C, Valori CF, Ahsan M, Wyles M, Higginbottom A, Herrmann T, Shaw P, Azzouz M, Sendtner M. 2010. PTEN depletion rescues axonal growth defect and improves survival in SMN-deficient motor neurons. *Hum Mol Genet* **19**: 3159–3168.

Noureddine MA, Donaldson TD, Thacker SA, Duronio RJ. 2002. Drosophila Roc1a encodes a RING-H2 protein with a unique function in processing the Hh signal transducer Ci by the SCF E3 ubiquitin ligase. *Dev Cell* **2**: 757–770.

Ogino S, Wilson RB. 2004. Spinal muscular atrophy: molecular genetics and diagnostics. *Expert Rev Mol Diagn* **4**: 15–29.

Ojeda L, Gao J, Hooten KG, Wang E, Thonhoff JR, Dunn TJ, Gao T, Wu P. 2011. Critical role of PI3k/Akt/GSK3β in motoneuron specification from human neural stem cells in response to FGF2 and EGF. *PLoS One* **6**.

Oprea GE, Kröber S, McWhorter ML, Rossoll W, Müller S, Krawczak M, Bassell GJ, Beattie CE, Wirth B. 2008. Plastin 3 is a protective modifier of autosomal recessive spinal muscular atrophy. *Science* **320**: 524–527.

Paquette N, Broemer M, Aggarwal K, Chen L, Husson M, Ertürk-Hasdemir D, Reichhart JM, Meier P, Silverman N. 2010. Caspase-Mediated Cleavage, IAP Binding, and Ubiquitination: Linking Three Mechanisms Crucial for Drosophila NF-κB Signaling. *Mol Cell* **37**: 172–182.

Passini MA, Bu J, Roskelley EM, Richards AM, Sardi SP, O'Riordan CR, Klinger KW, Shihabuddin LS, Cheng SH. 2010. CNS-targeted gene therapy improves survival and motor function in a mouse model of spinal muscular atrophy. *J Clin Invest* **120**: 1253.

Patton EE, Willems AR, Sa D, Kuras L, Thomas D, Craig KL, Tyers M. 1998. Cdc53 is a scaffold protein for multiple Cdc34/Skp1/F-box protein complexes that regulate cell division and methionine biosynthesis in yeast. *Genes Dev* **12**: 692–705.

Patton EE, Willems A, Tyers M. 1998. Combinatorial control in ubiquitin-dependent proteolysis: don't Skp the F-box hypothesis. *Trends Genet* **14**: 236–243.

Pearn J. 1980. Classification of Spinal Muscular Atrophies. *Lancet* 919–922.

Pellizzoni L, Yong J, Dreyfuss G. 2002. Essential role for the SMN complex in the specificity of snRNP assembly. *Science* **298**: 1775–1779.

Petroski MD. 2008. The ubiquitin system, disease, and drug discovery. *BMC Biochem* **9**.

Pillai RS, Grimmler M, Meister G, Will CL, Lührmann R, Fischer U, Schümperli D. 2003. Unique Sm core structure of U7 snRNPs: Assembly by a specialized SMN complex and the role of a new component, Lsm11, in histone RNA processing. *Genes Dev* **17**: 2321–2333.

Praveen K, Wen Y, Gray KM, Noto JJ, Patlolla AR, Van Duyne GD, Matera AG. 2014. SMA-Causing Missense Mutations in Survival motor neuron (Smn) Display a Wide Range of Phenotypes When Modeled in Drosophila. *PLoS Genet* **10**: e1004489.

Praveen K, Wen Y, Matera AG. 2012. A Drosophila model of spinal muscular atrophy uncouples snRNP biogenesis functions of survival motor neuron from locomotion and viability defects. *Cell Rep* **1**: 624–631.

Prior TW. 2010. Spinal muscular atrophy: a time for screening. *Curr Opin Pediatr* **22**: 696–702.

Rajendra TK, Gonsalvez GB, Walker MP, Shpargel KB, Salz HK, Matera AG. 2007. A Drosophila melanogaster model of spinal muscular atrophy reveals a function for SMN in striated muscle. *J Cell Biol* **176**: 831–841.

Ramser J, Ahearn ME, Lenski C, Yariz KO, Hellebrand H, von Rhein M, Clark RD, Rindt H, Feng Z, Mazzasette C, Glascock JJ, Valdivia D, Pyles N, Crawford TO,

Rogers SL, Rogers GC. 2008. Culture of Drosophila S2 cells and their use for RNAi-mediated loss-of-function studies and immunofluorescence microscopy. *Nat Protoc* **3**: 606–611.

Rossoll W, Jablonka S, Andreassi C, Kroning AK, Karle K, Monani UR, Sendtner M. 2003. Smn, the spinal muscular atrophy-determining gene product, modulates axon growth and localization of beta-actin mRNA in growth cones of motoneurons. *J Cell Biol* **163**: 801–812.

Sanchez G, Dury AY, Murray LM, Biondi O, Tadesse H, El Fatimy R, Kothary R, Charbonnier F, Khandjian EW. 2013. A novel function for the survival motoneuron protein as a translational regulator. *Hum Mol Genet* **22**: 668–684.

Sareen D, O'Rourke JG, Meera P, Muhammad AKMG, Grant S, Simpkinson M, Bell S, Carmona S, Ornelas L, Sahabian A, et al. 2013. Targeting RNA foci in iPSC-derived motor neurons from ALS patients with a C9ORF72 repeat expansion. *Sci Transl Med* **5**: 1-13.

Schmutzler RK, Lichtner P, Hoffman EP, et al. 2008. Rare Missense and Synonymous Variants in UBE1 Are Associated with X-Linked Infantile Spinal Muscular Atrophy. *Am J Hum Genet* **82**: 188–193.

Schrank B, Gotz R, Gunnersen JM, Ure JM, Toyka KV, Smith AG, Sendtner M. 1997. Inactivation of the survival motor neuron gene, a candidate gene for human spinal muscular atrophy, leads to massive cell death in early mouse embryos. *Proc Natl Acad Sci* **94**: 9920–9925.

Shafey D, Côté PD, Kothary R. 2005. Hypomorphic Smn knockdown C2C12 myoblasts reveal intrinsic defects in myoblast fusion and myotube morphology. *Exp Cell Res* **311**: 49–61.

Sharma A, Lambrechts A, Hao LT, Le TT, Sewry CA, Ampe C, Burghes AHM, Morris GE. 2005. A role for complexes of survival of motor neurons (SMN) protein with gemins and profilin in neurite-like cytoplasmic extensions of cultured nerve cells. *Exp Cell Res* **309**: 185–197.

Svendsen CN, Borg MG, Armstrong RJ, Rosser AE, Chandran S, Ostenfeld T, Caldwell MA. 1998. A new method for the rapid and long term growth of human neural precursor cells. *J Neurosci Methods* **85**: 141–152.

Swoboda KJ, Patitucci TN, Ebert AD, et al. 2015. Astrocytes influence the severity of spinal muscular atrophy. *Hum Mol Genet* **24**: 4094–4102.

Tan JMM, Wong ESP, Kirkpatrick DS, Pletnikova O, Ko HS, Tay SP, Ho MWL, Troncoso J, Gygi SP, Lee MK, et al. 2008. Lysine 63-linked ubiquitination promotes the formation and autophagic clearance of protein inclusions associated with neurodegenerative diseases. *Hum Mol Genet* **17**: 431–439.

Tiziano FD, Melki J, Simard LR. 2013. Solving the puzzle of spinal muscular atrophy: what are the missing pieces? *Am J Med Genet A* **161A**: 2836–2845.

Trinkle-Mulcahy L, Boulon S, Lam YW, Urcia R, Boisvert FM, Vandermoere F, Morrice NA, Swift S, Rothbauer U, Leonhardt H, et al. 2008. Identifying specific protein interaction partners using quantitative mass spectrometry and bead proteomes. *J Cell Biol* **183**: 223–239.

Valori CF, Ning K, Wyles M, Mead RJ, Grierson AJ, Shaw PJ, Azzouz M. 2010. Systemic delivery of scAAV9 expressing SMN prolongs survival in a model of spinal muscular atrophy. *Sci Transl Med* **2**: 35–42.

van Wijk SJL, Timmers HTM. 2010. The family of ubiquitin-conjugating enzymes (E2s): deciding between life and death of proteins. *FASEB J* **24**: 981–993.

Voigt T, Meyer K, Baum O, Schümperli D. 2010. Ultrastructural changes in diaphragm neuromuscular junctions in a severe mouse model for Spinal Muscular Atrophy and their prevention by bifunctional U7 snRNA correcting SMN2 splicing. *Neuromuscul Disord* **20**: 744–752.

Walker MP, Rajendra TK, Saieva L, Fuentes JL, Pellizzoni L, Matera AG. 2008. SMN complex localizes to the sarcomeric Z-disc and is a proteolytic target of calpain. *Hum Mol Genet* **17**: 3399–3410.

Wee CD, Kong L, Sumner CJ. 2010. The genetics of spinal muscular atrophies. *Curr Opin Neurol* **23**: 450–458.

Wirth B. 2000. An update of the mutation spectrum of the survival motor neuron gene (SMN1) in autosomal recessive spinal muscular atrophy (SMA). *Hum Mutat* **15**: 228–237.

Wishart TM, Mutsaers CA, Riessland M, Reimer MM, Hunter G, Hannam ML, Eaton SL, Fuller HR, Roche SL, Somers E, et al. 2014. Dysregulation of ubiquitin homeostasis and β-catenin signaling promote spinal muscular atrophy. *J Clin Invest* **124**: 1821–1834.

Ye Y, Rape M. 2009. Building ubiquitin chains: E2 enzymes at work. *Nat Rev Mol Cell Biol* **10**: 755–764.

Zhang L, Xu M, Scotti E, Chen ZJ, Tontonoz P. 2013. Both K63 and K48 ubiquitin linkages signal lysosomal degradation of the LDL receptor. *J Lipid Res* **54**: 1410–1420.

Zheng N, Schulman BA, Song L, Miller JJ, Jeffrey PD, Wang P, Chu C, Koepp DM, Elledge SJ, Pagano M, et al. 2002. Structure of the Cul1-Rbx1-Skp1-F boxSkp2 SCF ubiquitin ligase complex. *Nature* **416**: 703–709.

Zhou R, Silverman N, Hong M, Liao DS, Chung Y, Chen ZJ, Maniatis T. 2005. The role of ubiquitination in Drosophila innate immunity. *J Biol Chem* **280**: 34048–34055.

A

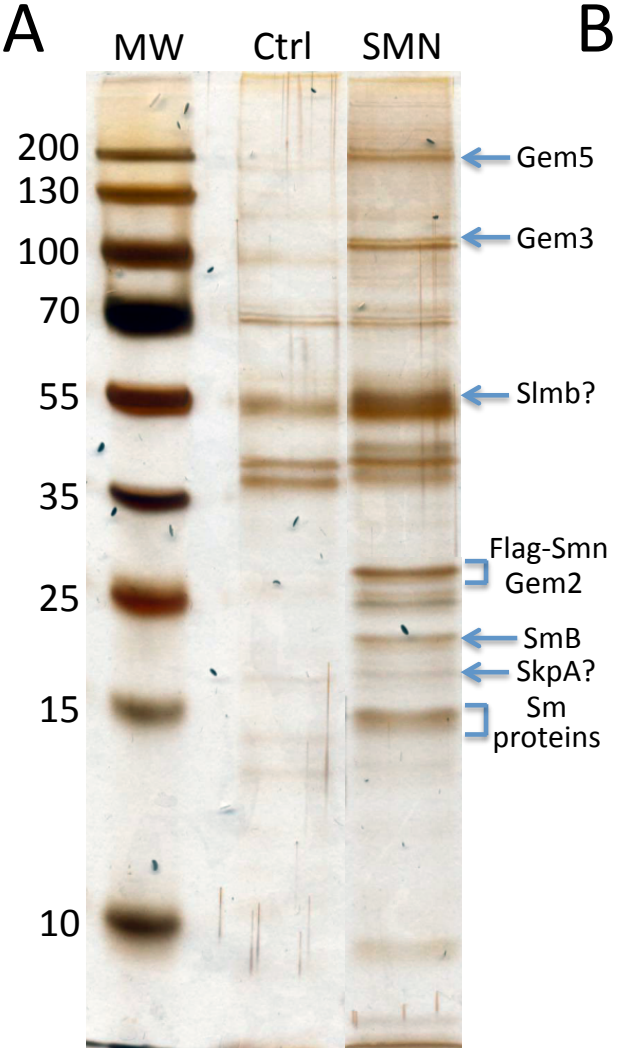

B

Protein	Gene #	Category	Intensity Ctrl (x10^5)	Intensity SMN (x10^5)	Peptides
Known SMN Interactors					
SMN	CG16725	SMN Complex	38.7	1415.2	9
Gem3	CG6539	SMN Complex	31.0	1052.2	31
Gem2	CG10419	SMN Complex	0.0	372.6	5
Gem5	CG30149	SMN Complex	0.0	96.5	16
SmE	CG18591	Sm protein	0.9	439.8	3
SmG	CG9742	Sm protein	0.4	364.5	6
SmD2	CG1249	Sm protein	0.0	303.4	5
SmF	CG16792	Sm protein	0.0	89.9	4
Lsm11	CG12924	Sm protein	0.0	47.3	8
SmD3	CG8427	Sm protein	0.3	31.1	2
SmD1	CG10753	Sm protein	0.0	20.0	3
Lsm10	CG12938	Sm protein	0.0	11.2	2
Novel UPS-associated Candidates					
Slmb	CG3412	UPS - SCF E3	0.7	253.6	13
SkpA	CG16983	UPS - SCF E3	3.4	91.1	5
Ben	CG18319	UPS - E2	2.1	27.3	5
Ubc2	CG6720	UPS - E2	2.9	9.2	2
Cul1	CG1877	UPS - SCF E3	0.0	8.0	4
UBE2S-like	CG8188	UPS - E2	0.0	5.8	3
Uch-L5	CG3431	UPS - DUB	1.1	4.5	2
Hyd	CG9484	UPS - E3	0.0	3.6	2
Cul5	CG1401	UPS - E3	0.0	2.8	2
Rpt1	CG1341	Proteasome	12.9	31.1	7
Rpt4	CG3455	Proteasome	8.8	29.2	6
Rpn2	CG11888	Proteasome	11.0	28.6	5
Rpn9	CG10230	Proteasome	6.5	23.0	5
Rpn6	CG10149	Proteasome	11.2	21.5	4
Rpn3	CG42641	Proteasome	2.7	15.3	5
Rpt3	CG16916	Proteasome	5.4	14.6	5
Rpn5	CG1100	Proteasome	6.0	13.2	4
Rpn11	CG18174	Proteasome	2.5	13.0	2
Rpn1	CG7762	Proteasome	1.9	11.0	5
Rpn7	CG5378	Proteasome	2.8	7.6	2
Rpn12	CG4157	Proteasome	2.5	5.2	3
CSN7	CG2038	COP9 signalosome	0.8	5.4	3
CSN3	CG18332	COP9 signalosome	0.0	3.7	2
CSN4	CG8725	COP9 signalosome	0.0	2.9	2
Sgg	CG2621	Kinase	2.2	9.8	4

C

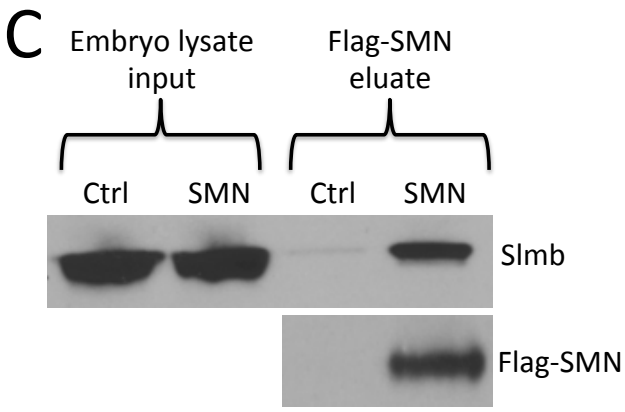

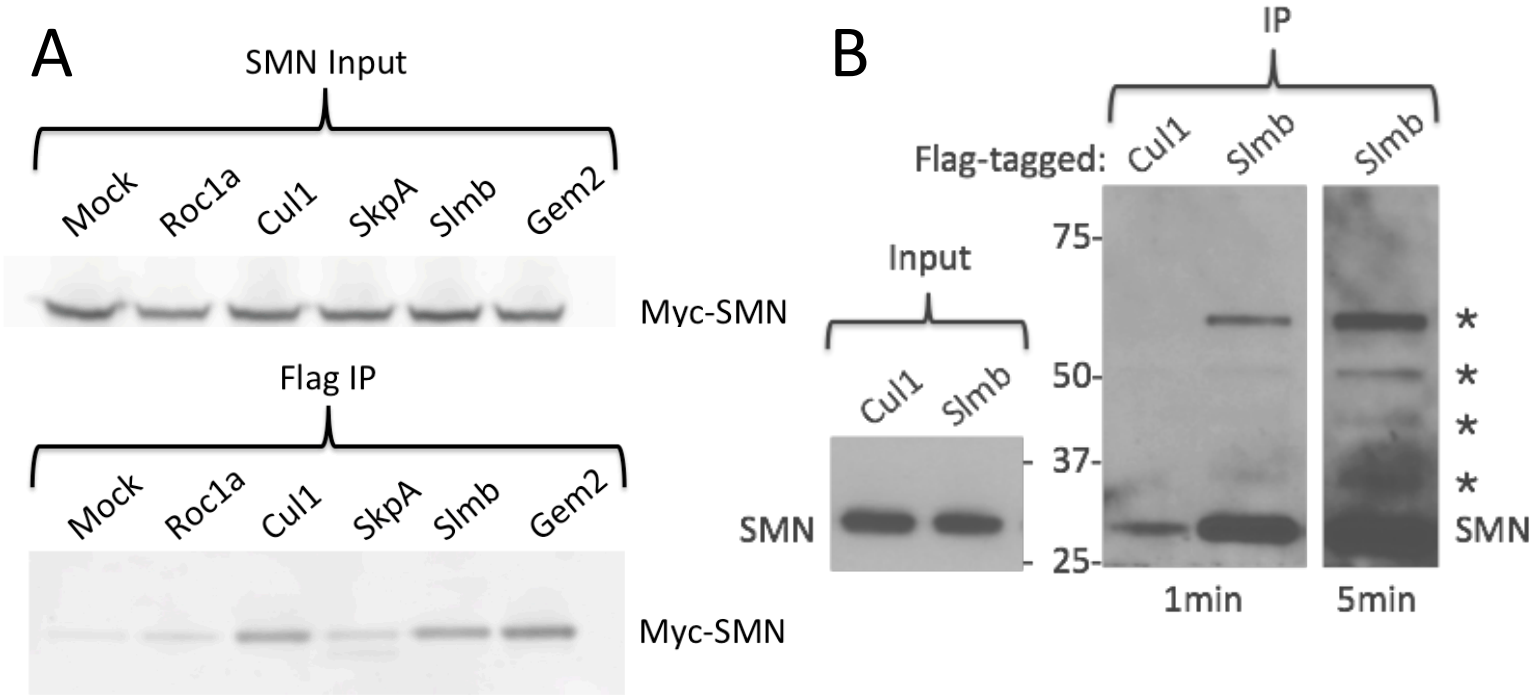

Drosophila S2 cells

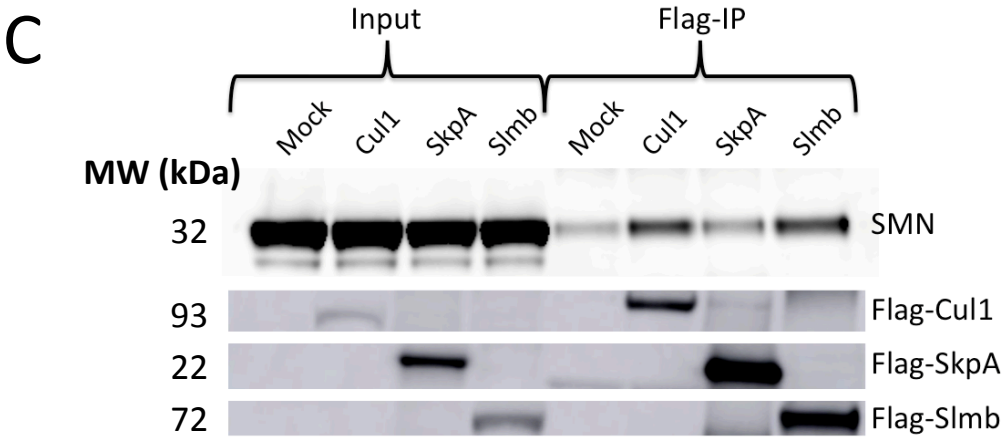

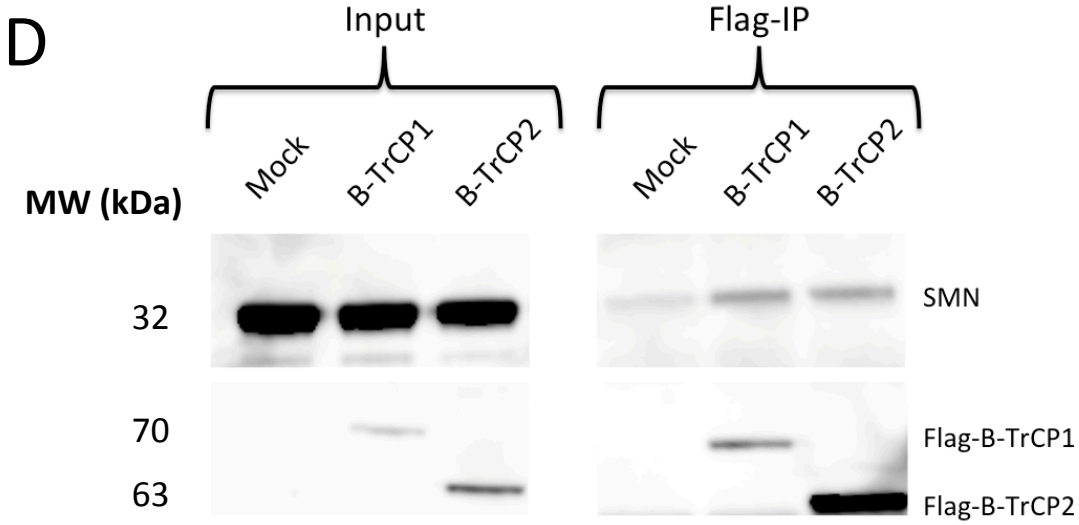

Human HEK293T cells

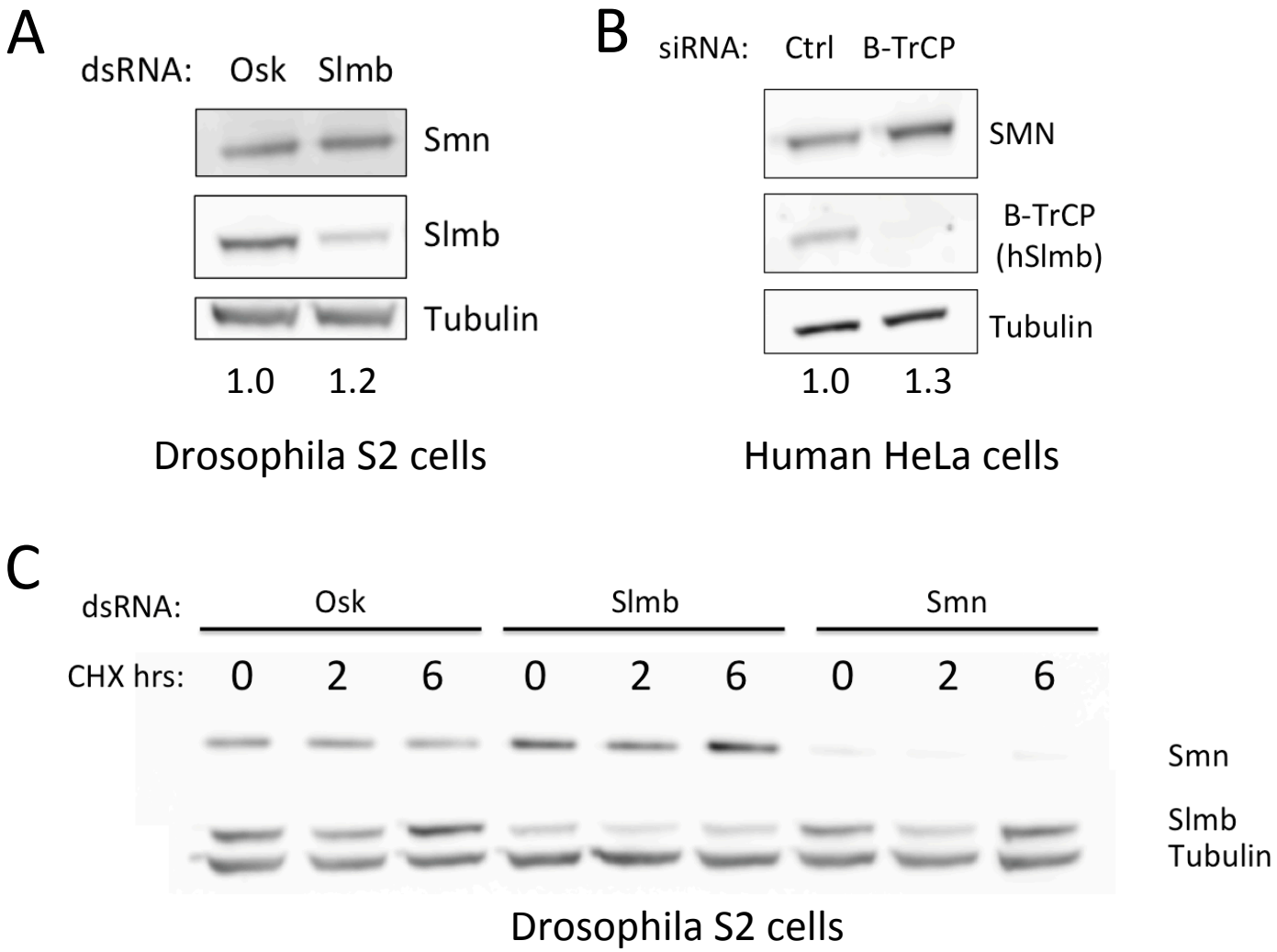

A

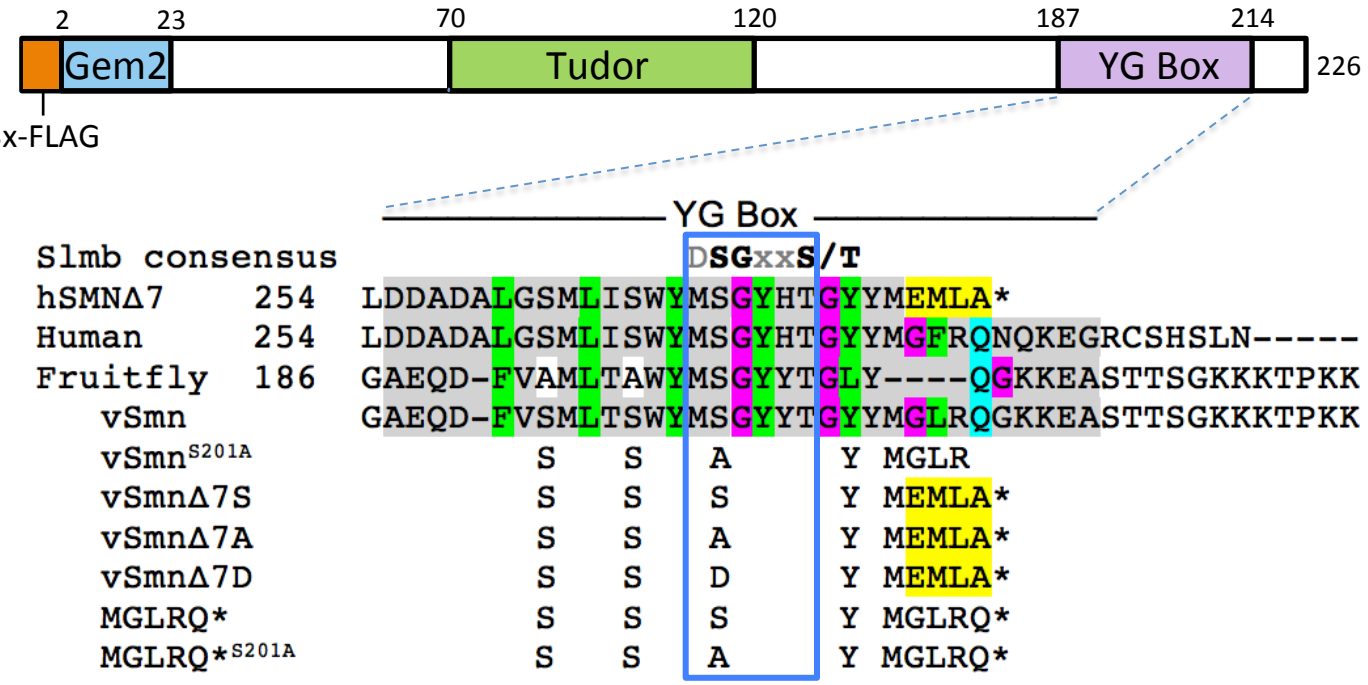

B

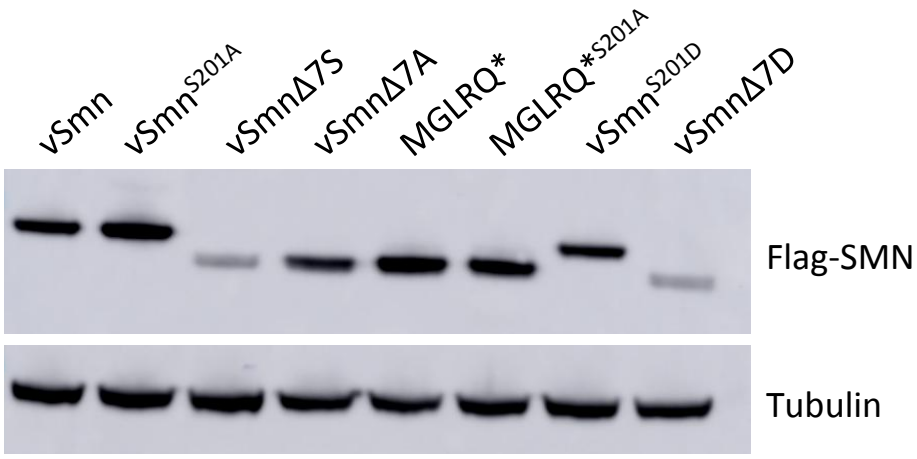

Normalized SMN levels: 1.0 1.3 0.1 0.4 1.2 1.3 0.7 0.2

C

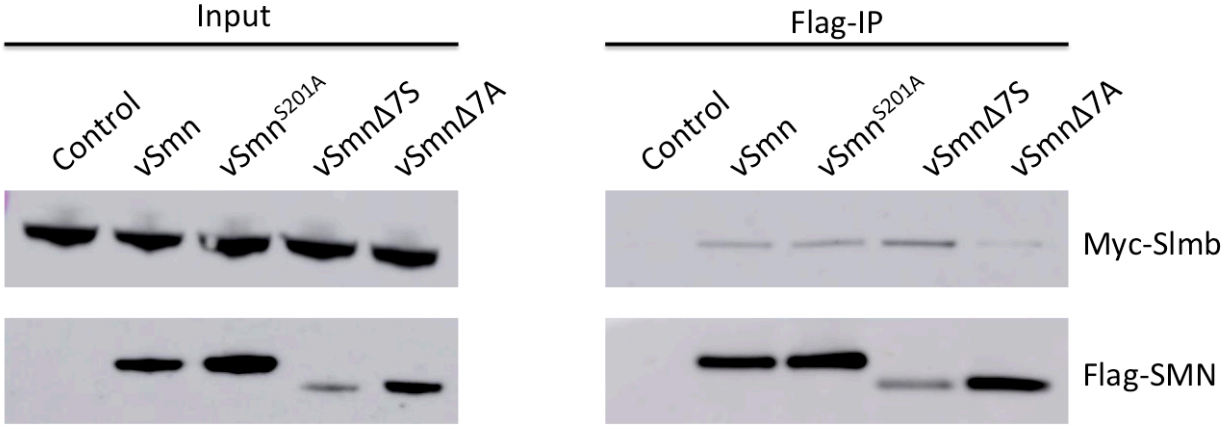

Relative binding (fold): 1.0 0.7 7.5 0.6

A

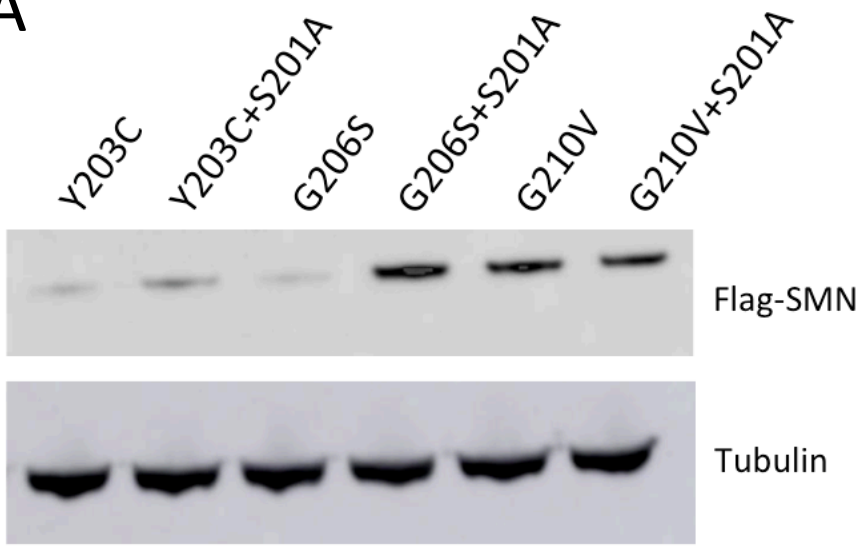
Y203C
Y203C+S201A
G206S
G206S+S201A
G210V
G210V+S201A
Flag-SMN
Tubulin

B

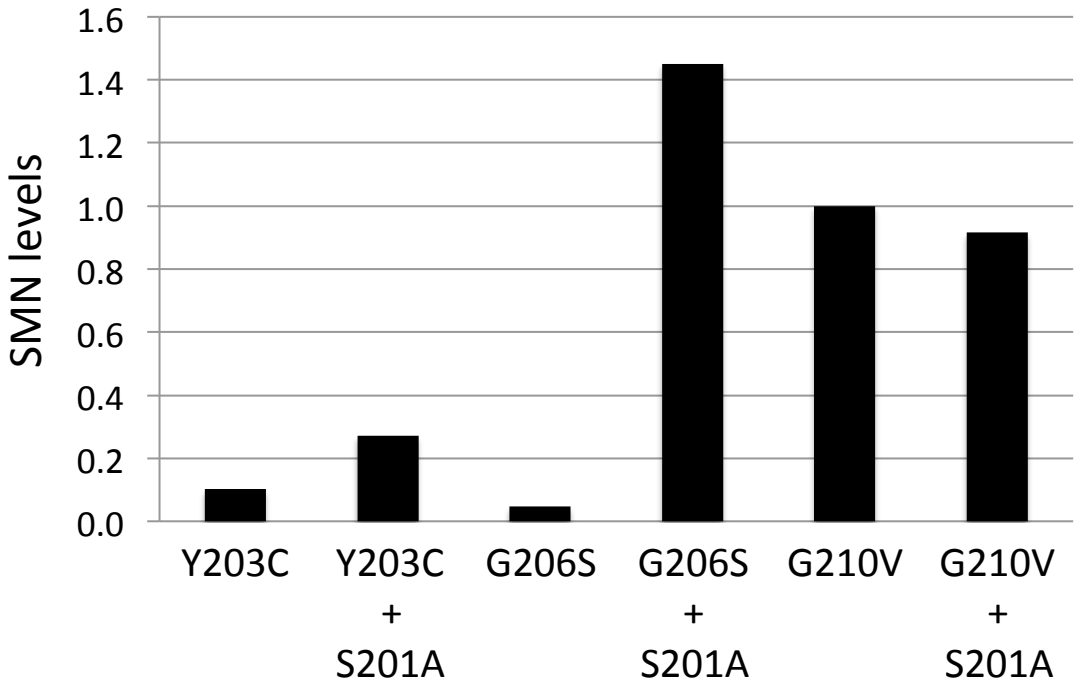
SMN levels
1.6
1.4
1.2
1.0
0.8
0.6
0.4
0.2
0.0
Y203C
Y203C + S201A
G206S
G206S + S201A
G210V
G210V + S201A

A

Genotype	Pupation (%)	Eclosion (%)
vSMN/–	86	83
$vSmn^{S201A}$/–	100	97.5
Smn^{WT}/–	99	73

n=200

B

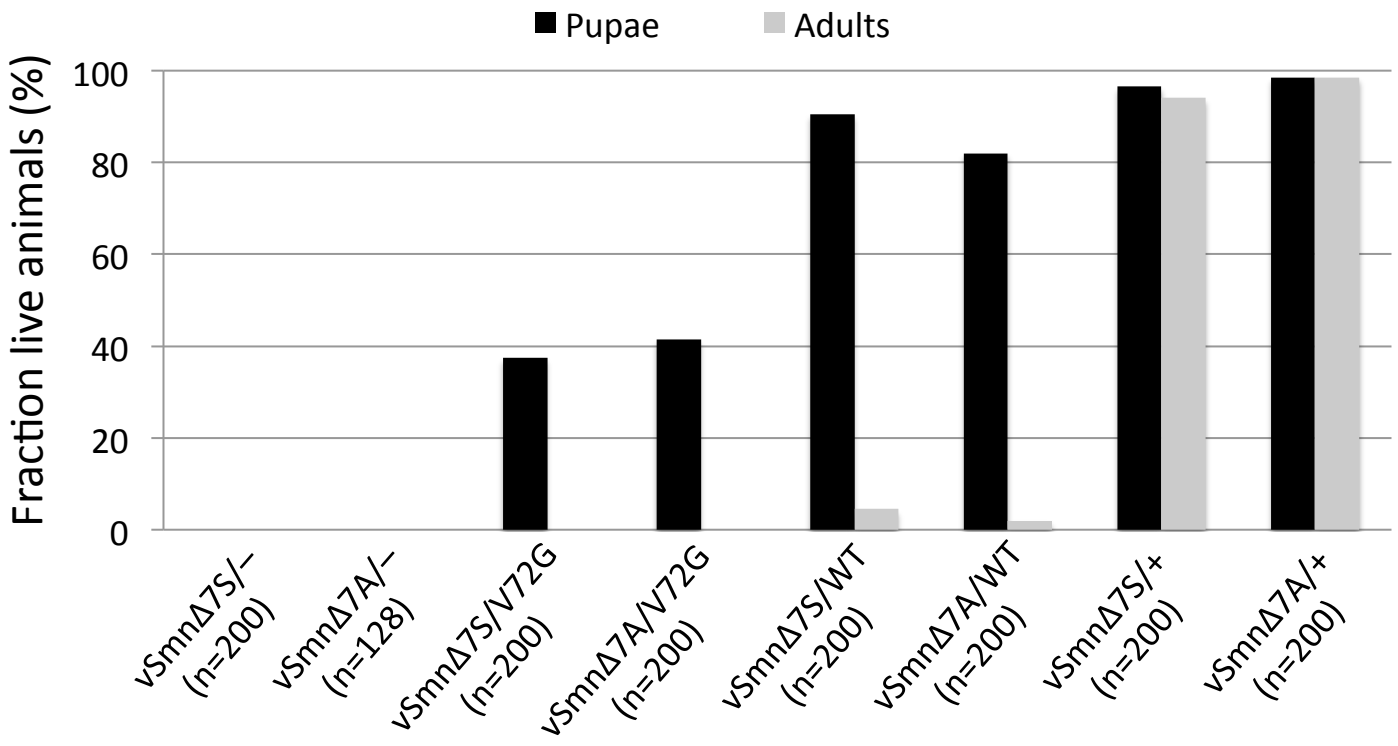

C

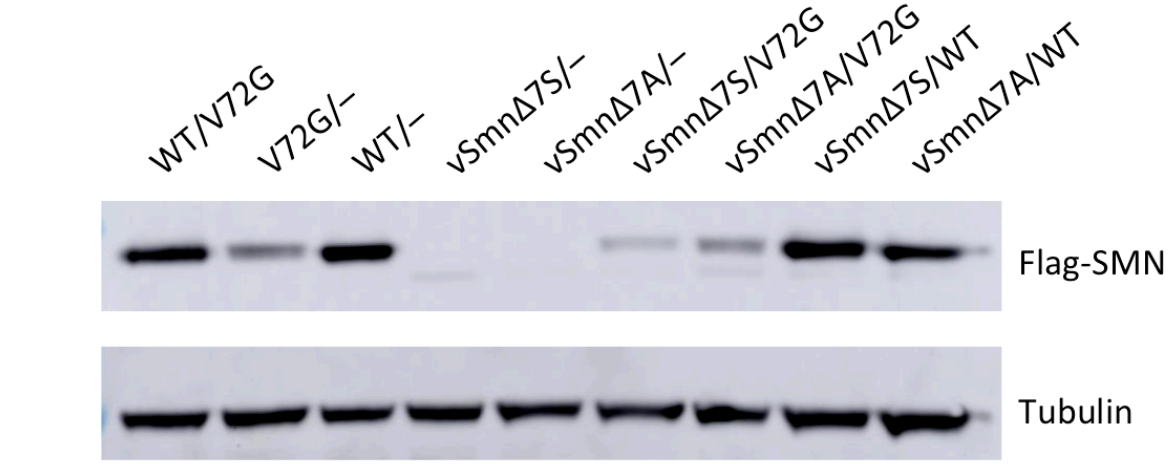

SMN: 1.0 0.4 1.5 – – 0.1 0.2 1.1 0.7

A

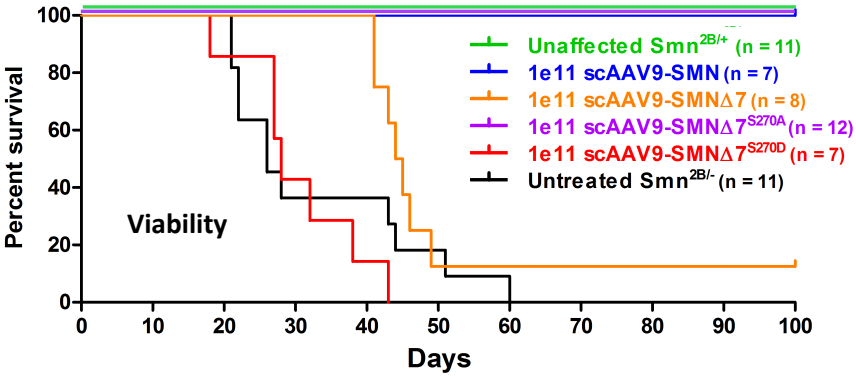
Percent survival
Days
Viability
Unaffected Smn2B/+ (n = 11)
1e11 scAAV9-SMN (n = 7)
1e11 scAAV9-SMNΔ7 (n = 8)
1e11 scAAV9-SMNΔ7S270A (n = 12)
1e11 scAAV9-SMNΔ7S270D (n = 7)
Untreated Smn2B/- (n = 11)

B

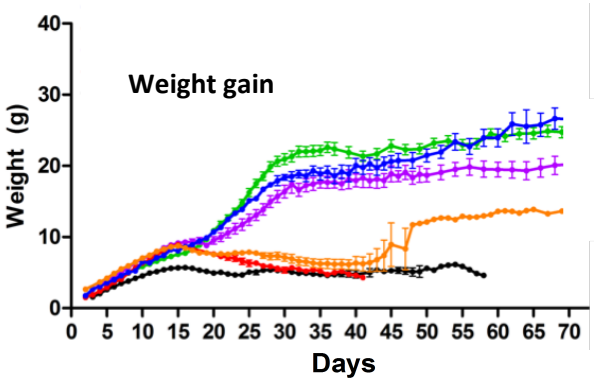
Weight gain
Weight (g)
Days

C

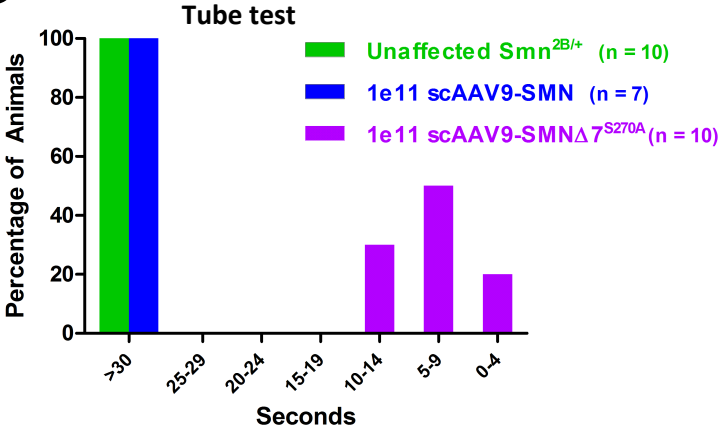
Tube test
Percentage of Animals
Unaffected Smn2B/+ (n = 10)
1e11 scAAV9-SMN (n = 7)
1e11 scAAV9-SMNΔ7S270A (n = 10)
>30
25-29
20-24
15-19
10-14
5-9
0-4
Seconds

D

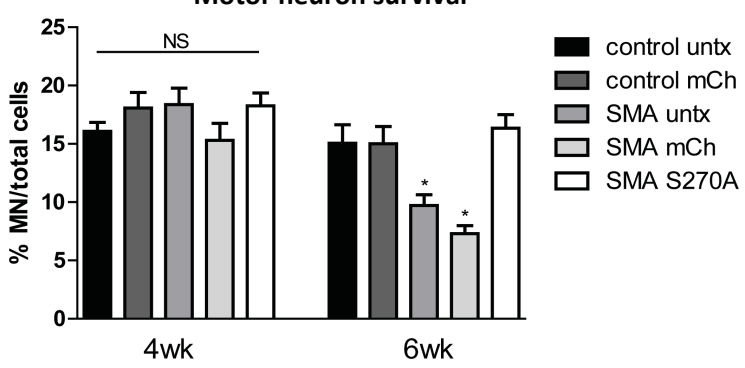
Motor neuron survival
% MN/total cells
NS
control untx
control mCh
SMA untx
SMA mCh
SMA S270A
4wk
6wk

E

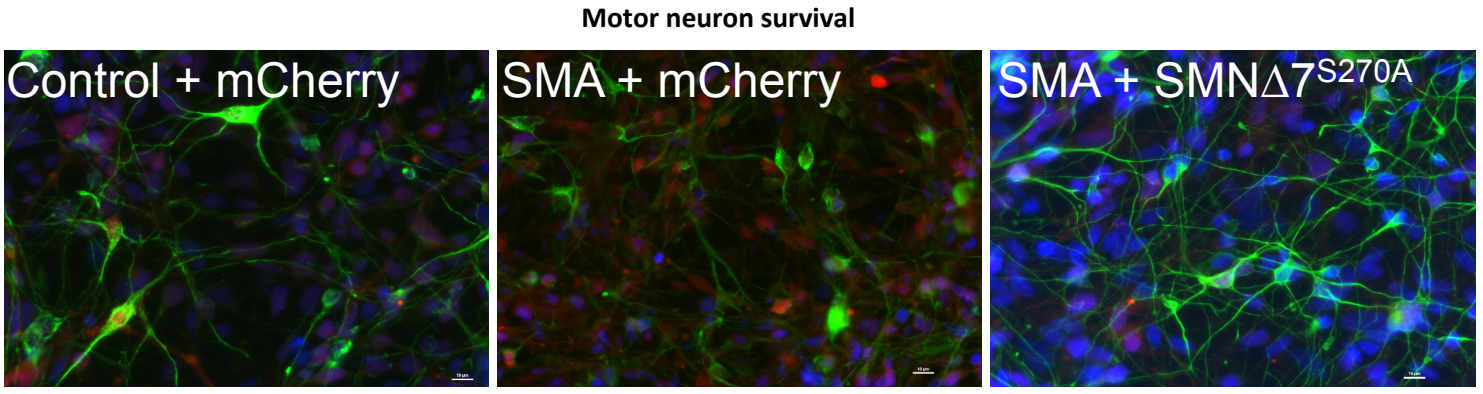
Motor neuron survival
Control + mCherry
SMA + mCherry
SMA + SMNΔ7S270A

S1

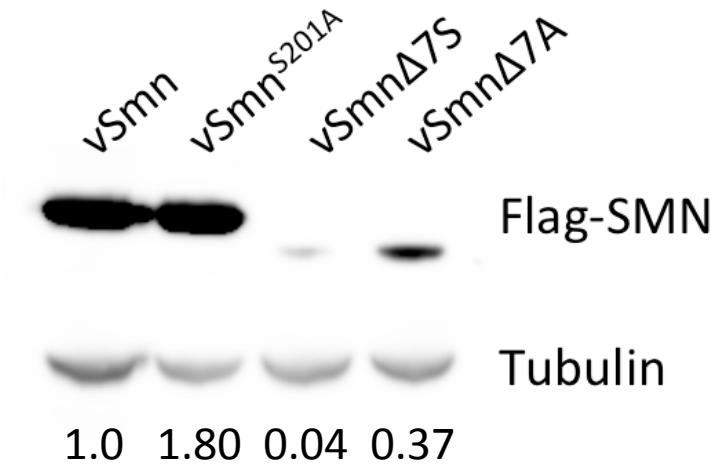
vSmn
vSmn^{S201A}
vSmnΔ7S
vSmnΔ7A
Flag-SMN
Tubulin
1.0 1.80 0.04 0.37

S2

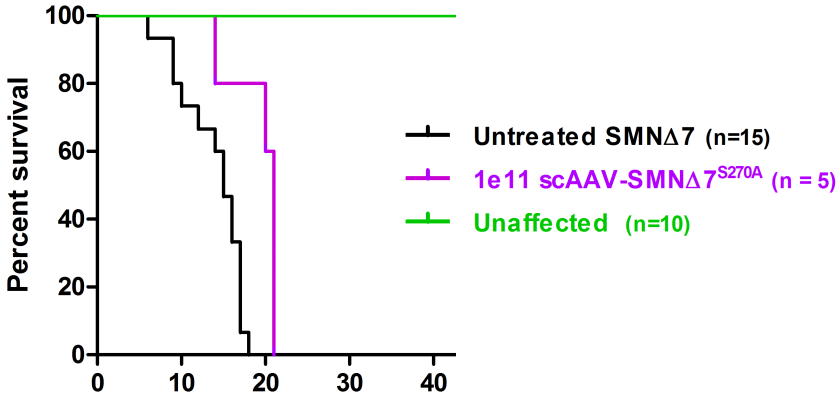
Percent survival
100
80
60
40
20
0
0 10 20 30 40
Untreated SMNΔ7 (n=15)
1e11 scAAV-SMNΔ7^{S270A} (n = 5)
Unaffected (n=10)

S3

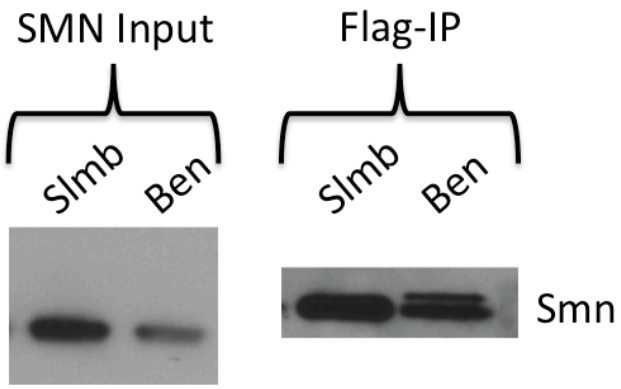
SMN Input
Flag-IP
Slmb
Ben
Slmb
Ben
Smn